(Santa Cruz, CA). Anti-mouse mast cell protease-8 mAb (TUG8) (Ugajin *et al.*, 2009) was provided by Dr Karasuyama of Tokyo Medical and Dental University.

Cutaneous inflammatory reactions

Trinitrophenyl (TNP)-specific IgE was purified from ascites of BALB/c-*nu/nu* mice by intraperitoneal injection of the IGEL b4 B cell hybridoma (ATCC, Rockville, MD; TIB141) (Rudolph *et al.*, 1981). IgE-CAI was induced by passive immunization of mice with TNP-specific IgE (150 μg per mouse, intravenous) (Mukai *et al.*, 2005). Mice were challenged 24 hours later with TNP-OVA (10 μg per ear, Biosearch Technologies, Novato, CA) on each ear lobe.

CHS reactions were induced by application of 50 μl of 0.5% DNFB (Nacalai Tesque, Kyoto, Japan) in acetone:olive oil (4:1) onto the ventral skin on day 0. On day 5, each ear lobe was challenged with 20 μl of 0.2% DNFB in acetone:olive oil (4:1). Ear thickness was measured using a dial thickness gauge (Ozaki, Tokyo, Japan) before and after the challenges.

DTH to SRBCs was induced by subcutaneous immunization with 100 μl of 20% SRBCs on the back on days −1 and 0. On day 5, 20 μl of 20% SRBC was injected into the footpad. Footpad thickness was measured before and after the challenges. Each group consisted of at least four mice.

Cell preparation

Primary basophils were prepared by enrichment of CD49b (+) cells from freshly isolated bone marrow cells using the MACS system with biotinylated anti-CD49b and streptavidin microbeads. As determined by flow cytometric analysis for CD49b and CD123 expression, the CD49b (+) cells included ~20% basophils.

Bone marrow–derived basophils were prepared by culturing bone marrow cells in RPMI 1640 supplemented with 10% fetal calf serum and 10 ng ml^{-1} rIL-3 (R&D Systems, Minneapolis, MN) for 10 days, followed by isolation of the CD49b (+) cells using an MACS system.

Bone marrow–derived mast cells were obtained by culturing bone marrow cells in the presence of 10 ng ml^{-1} rIL-3 for 4 weeks, followed by isolation of the c-kit+ cells.

Basophil transfer

Basophil transfer for inducing IgE-CAI in FcRγ chain(−/−) mice was performed using a previously described method (Mukai *et al.*, 2005). Briefly, CD49b (+) basophil–enriched bone marrow cells (primary basophils; 6×10^6 cells per recipient) were transferred into irradiated FcRγ(−/−) mice (6 Gy) together with CD49b(−) bone marrow cells (effector cells) from naive FcRγ chain(−/−) mice. Four days later, mice were passively immunized with TNP-IgE followed by challenge with TNP-OVA.

In vitro selectin binding assay of basophils

CD49b (+) basophil–enriched bone marrow cells were suspended in phosphate-buffered saline containing 5% fetal calf serum, 0.1% NaN_3, 1 mmol l^{-1} Ca^{2+}, and 1 mmol l^{-1} Mg^{2+}, followed by incubation with 10 μg ml^{-1} of murine P-, E-, or L-selectin-human IgG Fc chimera or control human IgG1 Fc (R&D Systems) for 40 minutes at 4 °C. After washing the cells, they were incubated with PE-F $(ab')_2$ goat anti-human IgG Fc Ab (Rockland, Gilbertsville, PA) for 30 minutes at 4 °C. They were then counterstained with FITC- FcεRI Ab or FITC- CD123 Abs. Selectin binding was examined using flow cytometric analysis with FACS Calibur (BD Biosciences, Mountain View, CA).

Real-time PCR

Quantitative real-time reverse-transcriptase PCR was performed with reverse-transcribed RNA by real-time monitoring of the increase in fluorescence of the SYBR Green dye (Brilliant SYBR Green QPCR Master Mix, Stratagene, La Jolla, CA) using the Mx3000P Real-Time PCR system (Stratagene). The primers for PCR were 5′-TGTGTCCGTC GTGGATCTGA-3′ and 5′-TTGCTGTTGAAGTCGCAGGAG-3′ for mouse GAPDH; 5′-CGCTGTGGGACCAATCTTGA-3′ and 5′-CCAGT GTTTGGCACCAGCA-3′ for mouse FT-IV; and 5′-AGATGCCCTGG TGGGCTTTAG-3′ and 5′-TCAGCCATGGGTCAAGGTAAGTC-3′ for mouse FT-VII.

Statistical analyses

A Student's *t*-test was used to assess statistical significance of the differences between the mean values. Analysis of the data for the time-course changes of the skin responses was performed by using the repeated measures analysis of variance test, followed by either a Student's *t*-test or Scheffe's F test.

CONFLICT OF INTEREST

The authors state no conflict of interest.

ACKNOWLEDGMENTS

This work was partly supported by the Japan Society for the Promotion of Science (22591238) and by the grant of the Ministry of Health, Labor and Welfare (H-21-114 and H-22-179), Japan. We thank J.B. Lowe and J.T. Myers for providing FT-IV(−/−), FT-VII(−/−), and FT-IV(−/−)/VII(−/−) mice. We are also grateful to C. Miyagishi for technical assistance.

SUPPLEMENTARY MATERIAL

Supplementary material is linked to the online version of the paper at http://www.nature.com/jid

REFERENCES

Alon R, Fuhlbrigge RC, Finger EB *et al.* (1996) Interactions through L-selectin between leukocytes and adherent leukocytes nucleate rolling adhesions on selectins and VCAM-1 in shear flow. *J Cell Biol* 135:849–65

Guyer DA, Moore KL, Lynam EB *et al.* (1996) P-selectin glycoprotein ligand-1 (PSGL-1) is a ligand for L-selectin in neutrophil aggregation. *Blood* 88:2415–21

Homeister JW, Thall AD, Petryniak B *et al.* (2001) The alpha(1,3)fucosyltransferases FucT-IV and FucT-VII exert collaborative control over selectin-dependent leukocyte recruitment and lymphocyte homing. *Immunity* 15:115–26

Ito Y, Satoh T, Takayama K *et al.* (2011) Basophil recruitment and activation in inflammatory skin diseases. *Allergy* 66:1107–13

Kieffer JD, Fuhlbrigge RC, Armerding D *et al.* (2001) Neutrophils, monocytes, and dendritic cells express the same specialized form of PSGL-1 as do skin-homing memory T cells: cutaneous lymphocyte antigen. *Biochem Biophys Res Commun* 285:577–87

Kobzdej MM, Leppanen A, Ramachandran V *et al.* (2002) Discordant expression of selectin ligands and sialyl Lewis x-related epitopes on murine myeloid cells. *Blood* 100:4485–94

Lee JJ, McGarry MP (2007) When is a mouse basophil not a basophil? *Blood* 109:859–61

Ley K, Bullard DC, Arbones ML *et al.* (1995) Sequential contribution of L- and P-selectin to leukocyte rolling *in vivo*. *J Exp Med* 181:669–75

Ley K, Tedder TF (1995) Leukocyte interactions with vascular endothelium. New insights into selectin-mediated attachment and rolling. *J Immunol* 155:525–8

Ley K, Tedder TF, Kansas GS (1993) L-selectin can mediate leukocyte rolling in untreated mesenteric venules *in vivo* independent of E- or P-selectin. *Blood* 82:1632–8

Lowe JB (2002) Glycosylation in the control of selectin counter-receptor structure and function. *Immunol Rev* 186:19–36

Luscinskas FW, Kansas GS, Ding H *et al.* (1994) Monocyte rolling, arrest and spreading on IL-4-activated vascular endothelium under flow is mediated via sequential action of L-selectin, beta 1-integrins, and beta 2-integrins. *J Cell Biol* 125:1417–27

Maly P, Thall A, Petryniak B *et al.* (1996) The alpha(1,3)fucosyltransferase Fuc-TVII controls leukocyte trafficking through an essential role in L-, E-, and P-selectin ligand biosynthesis. *Cell* 86:643–53

Mukai K, Matsuoka K, Taya C *et al.* (2005) Basophils play a critical role in the development of IgE-mediated chronic allergic inflammation independently of T cells and mast cells. *Immunity* 23:191–202

Obata K, Mukai K, Tsujimura Y *et al.* (2007) Basophils are essential initiators of a novel type of chronic allergic inflammation. *Blood* 110:913–20

Redrup AC, Howard BP, MacGlashan DW Jr *et al.* (1998) Differential regulation of IL-4 and IL-13 secretion by human basophils: their relationship to histamine release in mixed leukocyte cultures. *J Immunol* 160:1957–64

Rudolph AK, Burrows PD, Wabl MR (1981) Thirteen hybridomas secreting hapten-specific immunoglobulin E from mice with Iga or Igb heavy chain haplotype. *Eur J Immunol* 11:527–9

Satoh T, Kanai Y, Wu MH *et al.* (2005) Synthesis of {alpha}(1,3) fucosyltransferases IV- and VII-dependent eosinophil selectin ligand and recruitment to the skin. *Am J Pathol* 167:787–96

Smithson G, Rogers CE, Smith PL *et al.* (2001) Fuc-TVII is required for T helper 1 and T cytotoxic 1 lymphocyte selectin ligand expression and recruitment in inflammation, and together with Fuc-TIV regulates naive T cell trafficking to lymph nodes. *J Exp Med* 194:601–14

Sokol CL, Barton GM, Farr AG *et al.* (2008) A mechanism for the initiation of allergen-induced T helper type 2 responses. *Nat Immunol* 9:310–8

Sokol CL, Chu NQ, Yu S *et al.* (2009) Basophils function as antigen-presenting cells for an allergen-induced T helper type 2 response. *Nat Immunol* 10:713–20

Sperandio M, Smith ML, Forlow SB *et al.* (2003) P-selectin glycoprotein ligand-1 mediates L-selectin-dependent leukocyte rolling in venules. *J Exp Med* 197:1355–63

Spertini O, Luscinskas FW, Gimbrone MA Jr *et al.* (1992) Monocyte attachment to activated human vascular endothelium in vitro is mediated by leukocyte adhesion molecule-1 (L-selectin) under nonstatic conditions. *J Exp Med* 175:1789–92

Spertini O, Luscinskas FW, Kansas GS *et al.* (1991) Leukocyte adhesion molecule-1 (LAM-1, L-selectin) interacts with an inducible endothelial cell ligand to support leukocyte adhesion. *J Immunol* 147:2565–73

Takai T, Li M, Sylvestre D *et al.* (1994) FcR gamma chain deletion results in pleiotrophic effector cell defects. *Cell* 76:519–29

Tsujimura Y, Obata K, Mukai K *et al.* (2008) Basophils play a pivotal role in immunoglobulin-G-mediated but not immunoglobulin-E-mediated systemic anaphylaxis. *Immunity* 28:581–9

Tu L, Delahunty MD, Ding H *et al.* (1999) The cutaneous lymphocyte antigen is an essential component of the L-selectin ligand induced on human vascular endothelial cells. *J Exp Med* 189:241–52

Ugajin T, Kojima T, Mukai K *et al.* (2009) Basophils preferentially express mouse mast cell protease 11 among the mast cell tryptase family in contrast to mast cells. *J Leukoc Biol* 86:1417–25

Voehringer D (2009) The role of basophils in helminth infection. *Trends Parasitol* 25:551–6

von Bubnoff D, Novak N, Kraft S *et al.* (2003) The central role of FcepsilonRI in allergy. *Clin Exp Dermatol* 28:184–7

Wada T, Ishiwata K, Koseki H *et al.* (2010) Selective ablation of basophils in mice reveals their nonredundant role in acquired immunity against ticks. *J Clin Invest* 120:2867–75

Walcheck B, Moore KL, McEver RP *et al.* (1996) Neutrophil-neutrophil interactions under hydrodynamic shear stress involve L-selectin and PSGL-1. A mechanism that amplifies initial leukocyte accumulation of P-selectin *in vitro*. *J Clin Invest* 98:1081–7

Watanabe M, Satoh T, Yamamoto Y *et al.* (2008) Overproduction of IgE induces macrophage-derived chemokine (CCL22) secretion from basophils. *J Immunol* 181:5653–9

Weninger W, Ulfman LH, Cheng G *et al.* (2000) Specialized contributions by alpha(1,3)-fucosyltransferase-IV and FucT-VII during leukocyte rolling in dermal microvessels. *Immunity* 12:665–76

Yanaba K, Kaburagi Y, Takehara K *et al.* (2003) Relative contributions of selectins and intercellular adhesion molecule-1 to tissue injury induced by immune complex deposition. *Am J Pathol* 162:1463–73

Immunity
Article

Inflammatory Monocytes Recruited to Allergic Skin Acquire an Anti-inflammatory M2 Phenotype via Basophil-Derived Interleukin-4

Mayumi Egawa,[1,6] Kaori Mukai,[1,4,6] Soichiro Yoshikawa,[1] Misako Iki,[1] Naofumi Mukaida,[3] Yohei Kawano,[1] Yoshiyuki Minegishi,[1,2,5] and Hajime Karasuyama[1,2,*]
[1]Department of Immune Regulation
[2]JST, CREST
Tokyo Medical and Dental University Graduate School of Medical and Dental Sciences, Tokyo 113-8519, Japan
[3]Division of Molecular Bioregulation, Cancer Research Institute, Kanazawa University, Kanazawa 920-1192, Japan
[4]Present address: Department of Pathology, Stanford University School of Medicine, Stanford, CA 94305, USA
[5]Present address: Department of Molecular Medicine, Institute for Genome Research, The University of Tokushima, Tokushima 770-8503, Japan
[6]These authors contributed equally to this work
*Correspondence: karasuyama.mbch@tmd.ac.jp
http://dx.doi.org/10.1016/j.immuni.2012.11.014

SUMMARY

Monocytes and macrophages are important effectors and regulators of inflammation, and both can be divided into distinct subsets based on their phenotypes. The developmental and functional relationship between individual subsets of monocytes and those of macrophages has not been fully elucidated, although Ly6C$^+$CCR2$^+$ inflammatory and Ly6C$^-$CCR2$^-$ resident monocytes are generally thought to differentiate into M1 (classically activated) and M2 (alternatively activated) macrophages, respectively. Here we show that inflammatory monocytes recruited to allergic skin acquired an M2-like phenotype in response to basophil-derived interleukin-4 (IL-4) and exerted an anti-inflammatory function. CCR2-deficient mice unexpectedly displayed an exacerbation rather than alleviation of allergic inflammation, in spite of impaired recruitment of inflammatory monocytes to skin lesions. Adoptive transfer of inflammatory monocytes from wild-type but not IL-4 receptor-deficient mice dampened the exacerbated inflammation in CCR2-deficient mice. Thus, inflammatory monocytes can be converted from being proinflammatory to anti-inflammatory under the influence of basophils in allergic reactions.

INTRODUCTION

Monocytes are circulating leukocytes that can differentiate into macrophages and dendritic cells after their migration to peripheral tissues (Auffray et al., 2009; Domínguez and Ardavín, 2010; Geissmann et al., 2010; Shi and Pamer, 2011). Monocytes, macrophages, and dendritic cells are essential components of the innate immune system and participate in clearance of dead cells and pathogens, tissue healing, and initiation and regulation of the adaptive immunity. They can also contribute to the pathogenesis of inflammatory disorders. Accumulating evidence indicates that those cell types can be further divided into phenotypically distinct subsets, and each subset might have particular function in the steady state and inflammation (Auffray et al., 2009; Geissmann et al., 2010; Gordon and Taylor, 2005; Mosser and Edwards, 2008; Shi and Pamer, 2011).

Circulating monocytes commonly express CD115 (CSF1 receptor) on their surface and are divided into subsets on the basis of the expression of particular surface molecules including chemokine receptors (Auffray et al., 2009; Gordon and Taylor, 2005). In humans, differential expression of CD14 and CD16 allowed monocytes to be divided into two subsets: CD14$^+$ CD16$^-$ and CD14$^+$CD16$^+$ monocytes (Passlick et al., 1989). The former cells represent 80%–90% of blood monocytes, express high amounts of the chemokine receptor CCR2 and low amounts of CX3CR1, and are often called classical monocytes. By contrast, the latter (nonclassical) cells express high amounts of CX3CR1 and low amounts of CCR2 and can be further divided into at least two populations based on the expression of CD14 and CD64. Also in mice, two subsets of monocytes have been described (Auffray et al., 2009; Geissmann et al., 2003). The main subset of murine monocytes expresses Ly6C, CCR2, and low amounts of CX3CR1, suggesting that they are phenotypically equivalent to human CD14$^+$CD16$^-$ monocytes. Ly6C$^+$CCR2$^+$ monocytes are readily recruited to affected tissues where they produce inflammatory cytokines such as tumor necrosis factor-α (TNF-α) and IL-1 during infection and inflammation, and they were therefore termed "inflammatory" monocytes. The second subset of murine monocytes is characterized by high expression of CX3CR1 and the lack of Ly6C and CCR2 expression and were termed "resident" monocytes because they have a longer half-life and are found in both resting and inflamed tissues. They adhere to and migrate along the luminal surface of endothelial cells that line small blood vessels and therefore appear to patrol the endothelium in the steady state (Auffray et al., 2007).

Macrophages are also heterogeneous in their phenotype and function, depending on the signals they receive (Biswas and

Mantovani, 2010; Gordon and Taylor, 2005; Mosser and Edwards, 2008; Murray and Wynn, 2011). Classically activated M1-type macrophages are generated by stimulation with bacterial moieties such as lipopolysaccharide (LPS) and the Th1 cell cytokine interferon-γ (IFN-γ), whereas alternatively activated M2-type macrophages are typically elicited by stimulation with the Th2 cell cytokines such as IL-4 and IL-13. M1 macrophages produce proinflammatory cytokines including IL-1 and destroy intracellular pathogens such as *M. tuberculosis* by means of an increased oxidative burst and NO production. Although the in vivo roles of M2 macrophages have been less well characterized, several functions are ascribed to them, including those in protection from parasitic infections, promoting Th2 cell-type immune responses, damping excessive inflammation, tumor progression, angiogenesis, wound healing, tissue remodeling, and fibrosis (Kreider et al., 2007; Martinez et al., 2009; Murray and Wynn, 2011).

The developmental and functional relationship between individual subsets of monocytes and those of macrophages has not been fully elucidated. It is generally thought that $Ly6C^+CCR2^+$ inflammatory monocytes exit the bone marrow in a CCR2-dependent manner and are recruited to inflamed tissues where they can differentiate to inflammatory M1 macrophages (Auffray et al., 2009; Dunay et al., 2008; Ingersoll et al., 2011; Serbina and Pamer, 2006; Tsou et al., 2007). In contrast, the differentiation of monocytes toward M2 macrophages remains ill defined. It has been suggested that $Ly6C^-CCR2^-$ resident monocytes are also recruited to sites of inflammation and then differentiate into M2 macrophages, contributing to wound healing (Auffray et al., 2007, 2009; Geissmann et al., 2010). Alternatively, recent study with a mouse model of helminth infection demonstrated that M2 macrophages are generated through IL-4-mediated proliferation and alternative activation of tissue-resident macrophages rather than the recruitment of blood monocytes (Jenkins et al., 2011). Thus, the origin of M2 macrophages and their mode of generation under homeostatic and pathological conditions remain obscure.

Basophils, the least common granulocyte, represent ~0.5% of peripheral blood leukocytes (Galli, 2000). Owing to their phenotypic similarities to mast cells and their small numbers, basophils had long been neglected in immunological studies. However, recent studies have defined previously unrecognized roles for basophils, including those in allergic responses, protection against parasitic infections, and regulation of acquired immunity (Karasuyama et al., 2011a; Min et al., 2012; Siracusa et al., 2011; Voehringer, 2011). Basophils readily generate large quantities of Th2 cell cytokines such as IL-4 and IL-13 (Piccinni et al., 1991; Seder et al., 1991), which contribute to initiation of Th2 cell differentiation (Perrigoue et al., 2009; Sokol et al., 2008, 2009; Yoshimoto et al., 2009) and to activation of B cells for the enhancement of humoral memory responses (Chen et al., 2009; Denzel et al., 2008). It remains to be investigated whether basophils and their products have any impact on the activation and differentiation of innate immune cells, including monocytes and macrophages.

In the present study, we analyzed the fate, polarization, and function of monocytes after their recruitment to skin lesions of immunoglobulin E (IgE)-mediated chronic allergic inflammation (IgE-CAI), a model where basophils rather than mast cells and T cells play a critical role for the elicitation of allergic response (Mukai et al., 2005). We found that $Ccr2^{-/-}$ mice unexpectedly displayed an exacerbation rather than alleviation of IgE-CAI, and ultimately identified a previously unappreciated mode of M2 generation, in that inflammatory monocytes can differentiate into anti-inflammatory M2-type macrophages via basophil-derived IL-4, which in turn dampen allergic inflammation.

RESULTS

$Ly6C^+CCR2^+$ Inflammatory Monocytes Are Recruited to Allergen-Exposed Skin in IgE-CAI

We previously showed that an intradermal administration of allergen induces three consecutive waves of ear swelling in mice sensitized with allergen-specific IgE, with peaks of swelling 30 min, 10 hr, and 3–4 days after the allergen challenge (Mukai et al., 2005). The delayed-onset (third) ear swelling with prominent inflammation was designated IgE-CAI (Mukai et al., 2005). Diphtheria toxin (DT)-mediated basophil ablation before the antigen challenge abolished the development of IgE-CAI in $Mcpt8^{DTR}$ mice (Wada et al., 2010) as shown in Figure 1A. This confirmed the conclusion in our previous studies that basophils play a pivotal role in the initiation of IgE-CAI, based on the results of experiments via the cell transfer and antibody-mediated basophil depletion (Mukai et al., 2005; Obata et al., 2007). Flow cytometric analysis revealed that the cell number in the skin lesions increased during the progress of IgE-CAI (Figure 1B). Monocyte- and macrophage-lineage cells (referred to here as monocytes-macrophages) and eosinophils were the major cell types among the cellular infiltrates whereas neutrophils and basophils were much less abundant (Figure 1C).

The vast majority of monocytes-macrophages isolated from the IgE-CAI skin lesions expressed Ly6C and CCR2, in contrast to those isolated from the control ear skin (Figure 2A and Figure S1A available online). Although resident macrophages in ear skin of naive mice barely express Ly6C, substantial numbers of $Ly6C^+CCR2^+$ monocytes-macrophages were detectable in the skin lesions even at 1 day after challenge (Figure S1A, top). These results suggested that monocytes-macrophages accumulating in the skin lesions were derived from $Ly6C^+CCR2^+$ inflammatory monocytes circulating in the peripheral blood (Figure S1B). Among the skin-infiltrating cells examined, basophils also expressed relatively high amounts of CCR2 on their surface in both C57BL/6 and BALB/c mice (Figure 2B). The expression of mRNAs encoding CCR2 ligands CCL8 and CCL12 (but not CCL2) was upregulated in the IgE-CAI skin lesions (Figure 2C). Various types of cells in the skin lesions expressed the CCR2 ligands, but basophils showed little or no expression of any of them (Figure S2A). Based on these observations, we assumed that CCR2 could contribute to the recruitment of both basophils and inflammatory monocytes to the skin lesions and hence the development of IgE-CAI.

$Ccr2^{-/-}$ Mice Show Exacerbated IgE-CAI in Spite of Impaired Recruitment of Inflammatory Monocytes

In sharp contrast to our expectation, the ear swelling in IgE-CAI was greatly augmented and prolonged in $Ccr2^{-/-}$ mice compared to that in wild-type mice (Figure 3A). Histopathological

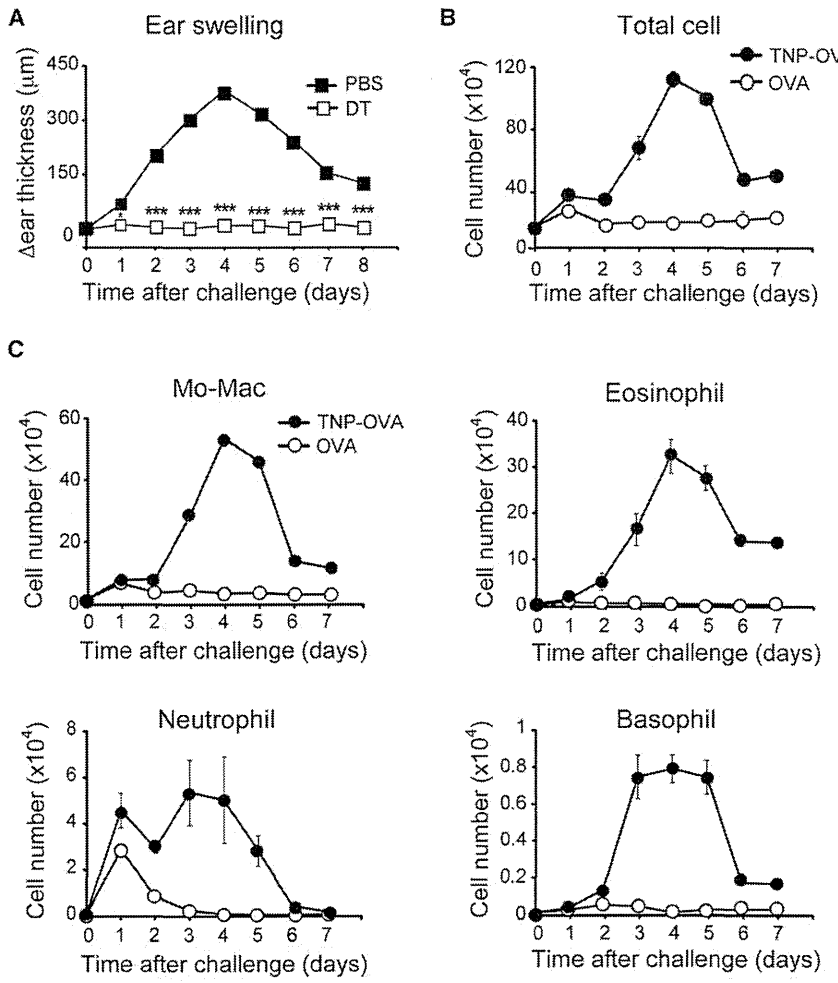

Figure 1. Cellular Components in the IgE-CAI Reaction that Is Elicited by Basophils

(A) *Mcpt8*^{DTR} C57BL/6 mice were sensitized with anti-TNP IgE and challenged with intradermal administration of TNP-OVA (or control OVA) in their ears to induce IgE-CAI. The mice were treated with either DT (open squares) or control PBS (closed squares) twice, 1 day before and 3 days after the antigen challenge. Time course of ear swelling (Δear thickness) is shown (mean ± SEM, n = 5 each). *$p < 0.05$, ***$p < 0.001$.

(B and C) C57BL/6 mice were sensitized with anti-TNP IgE and challenged with TNP-OVA (closed circles) or control OVA (open circles). The number of total cells (B) and indicated cell types (C) isolated from the ear skin at each time point postchallenge is shown (mean ± SEM, n = 3 each).

Data shown are representative of at least three independent experiments. Note that error bars are displayed in all figures, but often are hidden behind symbols such as squares and circles.

examination revealed many more cellular infiltrates in the skin lesion of *Ccr2*$^{-/-}$ mice (Figure 3B). Flow cytometric analysis demonstrated that the accumulation of monocytes-macrophages in the skin lesions was almost completely abolished in *Ccr2*$^{-/-}$ mice, as expected (Figure 3C). By contrast, the infiltration of basophils was enhanced rather than reduced in *Ccr2*$^{-/-}$ mice (Figure 3C), indicating that CCR2 was dispensable for the basophil recruitment, unlike for the monocyte recruitment. The accumulation of neutrophils in the skin lesions was also augmented in *Ccr2*$^{-/-}$ mice (Figure 3C). Thus, the IgE-CAI reaction was exacerbated rather than alleviated in *Ccr2*$^{-/-}$ mice, in spite of the fact that the recruitment of Ly6C^{+} inflammatory monocytes was abolished.

Monocytes-Macrophages in the Skin Lesions Display a Combined Phenotype of Inflammatory Monocytes and M2 Macrophages

To clarify the reason for this unexpected observation, we further examined the phenotype of monocytes-macrophages infiltrating the IgE-CAI skin lesions of wild-type mice. Approximately two-thirds of them expressed programmed death 1 ligand 2 (PD-L2) on their surface, whereas few cells isolated from the control skin did so (Figures 4A, 4B, and S1A, bottom). Because PD-L2 is a marker of M2-type macrophages (Loke and Allison, 2003), we examined the expression of other M2 markers in the skin lesions during the IgE-CAI reaction. The *Arg1*, *Chi3l3*, and *Fizz1* expression was upregulated and then downregulated, in parallel with the number of PD-L2^{+} monocytes-macrophages in the skin lesions (Figures 4B and 4C). Moreover, PD-L2^{+} monocytes-macrophages expressed significantly higher amounts of these mRNAs compared to PD-L2^{-} monocytes-macrophages and other cell lineages in the IgE-CAI skin lesions (Figures 4D and S2B), demonstrating that PD-L2^{+} monocytes-macrophages indeed displayed an M2 phenotype.

Gene profiling of monocytes-macrophages accumulating in the skin lesions revealed that M2 markers (*Arg1*, *Chi3l3*, and *Fizz1*) but not M1 markers (*Il1b*, *Nos2*, and *Tnfa*) were significantly upregulated during the IgE-CAI progression (Figure S3A). By contrast, the expression of the M2 markers and PD-L2 in blood monocytes, regardless of Ly6C expression, remained undetectable or very low during the IgE-CAI progression (Figures S3C and S3D). Importantly, the expression of genes involved in the macrophage differentiation (*Maf* and *Mafb*) but not those involved in the dendritic cell differentiation (*Sfpi1* and *Relb*) was upregulated in monocytes-macrophages in the skin lesions during the IgE-CAI progression (Figure S3B). These results strongly suggested that inflammatory monocytes recruited to the skin lesions differentiated into M2- but not M1-type macrophages during the IgE-CAI reaction. In contrast, monocytes-macrophages accumulating in skin lesions of delayed-type hypersensitivity (DTH) to the same antigen displayed an M1 phenotype with little or no expression of M2 markers including PD-L2 (Figure S4). Thus, the phenotype of monocytes-macrophages in skin lesions, either M1 or M2, appeared to be

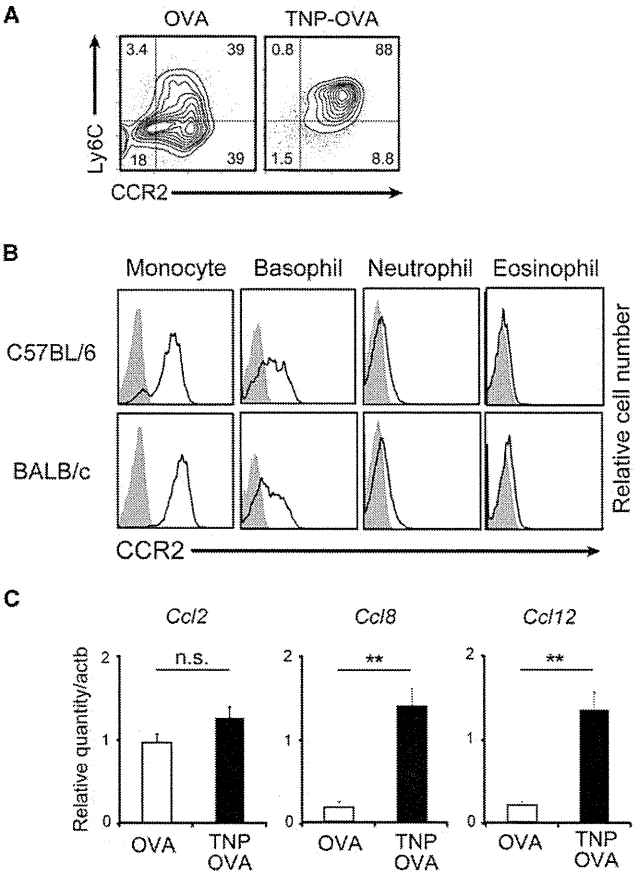

Figure 2. Monocytes-Macrophages Accumulating in the IgE-CAI Skin Lesions Display a Phenotype of Inflammatory Monocytes

(A) C57BL/6 mice were treated as in Figure 1 to induce IgE-CAI. The expression of Ly6C and CCR2 on F4/80$^+$CD11b$^+$SSC^{lo} monocytes-macrophages in the skin lesions of mice challenged with TNP-OVA or control OVA was examined on day 4 postchallenge.

(B) The expression of CCR2 on indicated cell lineages isolated from the bone marrow of C57BL/6 and BALB/c mice. Shaded histograms show control staining with isotype-matched antibody.

(C) The expression of indicated mRNAs in the skin lesions of mice challenged with TNP-OVA or control OVA was examined on day 3 postchallenge (mean ± SEM, n = 5 each).

Data shown are representative of three independent experiments. NS, not significant; **p < 0.01. See also Figures S1 and S2.

associated with the type of immune responses rather than the nature of antigens.

A previous study with a mouse model of helminth infection reported that M2 macrophages are generated through the proliferation and alternative activation of tissue-resident macrophages without any requirement of the blood monocyte recruitment (Jenkins et al., 2011). Therefore, we examined whether this mode of M2 generation could also take place in IgE-CAI. Although tissue-resident macrophages, mostly negative for Ly6C, were detected in ear skin of naive *Ccr2*$^{-/-}$ mice to an extent comparable to that observed in wild-type mice (Figure S5A), PD-L2$^+$ monocytes-macrophages were barely detected in the IgE-CAI skin lesions of *Ccr2*$^{-/-}$ mice (Figure 4E). Moreover, few monocytes-macrophages in the skin lesions of wild-type mice were positive for a proliferation marker Ki-67, regardless of the PD-L2 expression (Figure S5B). Thus, the proliferation and M2 conversion of tissue-resident macrophages appear to have little, if any, contribution to the M2 generation during the IgE-CAI reaction.

Basophil-Derived IL-4 Confers an M2-like Phenotype on Ly6C$^+$ Inflammatory Monocytes Ex Vivo

Th2 cell cytokines such as IL-4 and IL-13 as well as IL-10 have been shown to induce the differentiation of macrophages toward M2. Quantitative RT-PCR analysis revealed that the expression of *Il4* but not *Il13* or *Il10* mRNAs in the IgE-CAI skin lesions was upregulated in parallel with the accumulation of PD-L2$^+$ monocytes-macrophages (Figure 5A). *Il4* mRNAs were almost exclusively expressed by basophils among various cell types isolated from the skin lesions (Figure 5B). Indeed, primary basophils isolated from the bone marrow produced substantial amounts of IL-4 but not IL-13 when stimulated ex vivo with IgE plus antigens (Figure 5C).

Ly6C$^+$Ly6G$^-$ inflammatory monocytes freshly isolated from the bone marrow expressed no detectable PD-L2 on their surface (Figure 5D). Of note, they upregulated the PD-L2 expression when incubated ex vivo with the culture supernatants of primary basophils that had been stimulated with IgE plus antigens. This upregulation of PD-L2 was abolished when IL-4 antibody was included during the incubation (Figures 5D and 5E), indicating that basophil-derived IL-4 was responsible for the PD-L2 upregulation in inflammatory monocytes. The expression of *Arg1*, *Chi3l3*, and *Fizz1* mRNAs in inflammatory monocytes was also upregulated when incubated with the culture supernatants of activated basophils in an IL-4-dependent manner (Figure 5F). These results demonstrated that basophil-derived IL-4 can confer an M2-like phenotype on monocytes even before they differentiate into macrophages.

Skin-Infiltrating Monocytes Acquire an M2-like Phenotype in an IL-4R- and Basophil-Dependent Manner

We next examined whether the basophil IL-4-mediated acquisition of an M2-like phenotype by inflammatory monocytes indeed occurs in vivo. First, CD115$^+$ bone marrow monocytes were prepared from wild-type mice, labeled with CFSE, and adoptively transferred into IgE-sensitized wild-type mice, simultaneously with the challenge with allergens. On day 3 postchallenge, many of CFSE-labeled cells infiltrating the skin lesions became positive for PD-L2, concomitantly with F4/80 upregulation (Figure 6A), indicating their differentiation into M2-type macrophages. Of note, virtually all of the CFSE$^+$PD-L2$^+$F4/80$^+$ cells expressed Ly6C (Figure 6A), suggesting that they were derived from Ly6C$^+$ inflammatory but not Ly6C$^-$ resident monocytes. Indeed, when CD115$^+$Ly6C$^+$Ly6G$^-$ inflammatory monocytes were purified from the bone marrow and adoptively transferred, most of them became positive for PD-L2 in the skin lesions on day 3 postchallenge (Figure 6B).

Second, to examine the IL-4 dependency of M2 differentiation, CD115$^+$ bone marrow monocytes were prepared from wild-type or *Il4ra*$^{-/-}$ mice, labeled with CFSE, and adoptively transferred into wild-type mice, followed by IgE-CAI induction (Figure 6C). On day 1 postchallenge, when few basophils were recruited to the skin lesions (Figure 1C), little or no expression of PD-L2

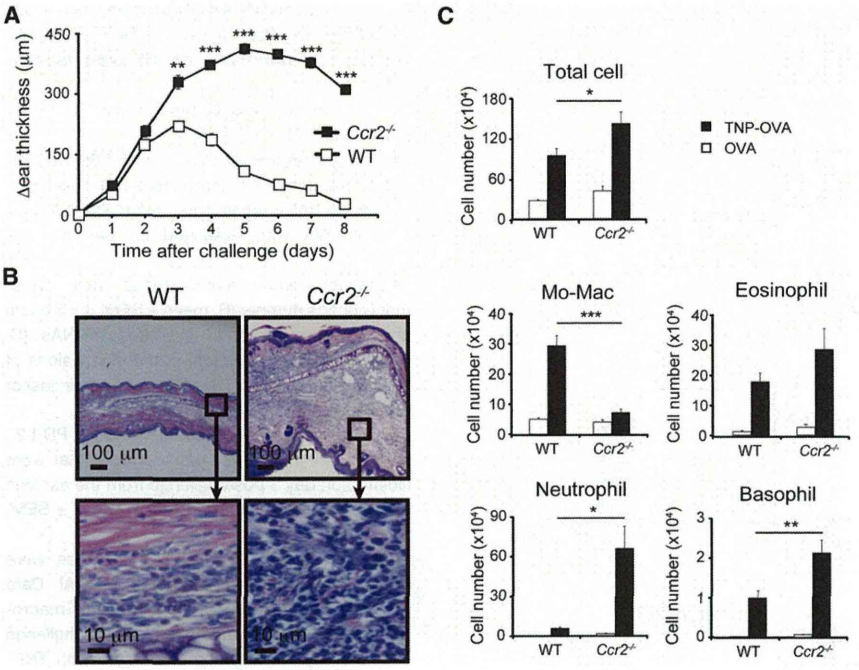

Figure 3. IgE-CAI Is Exacerbated rather than Ameliorated in *Ccr2*$^{-/-}$ Mice

Wild-type and *Ccr2*$^{-/-}$ BALB/c mice were treated as in Figure 1 to induce IgE-CAI.

(A) Time course of ear swelling (Δear thickness) in wild-type (open squares) and *Ccr2*$^{-/-}$ (closed squares) mice is shown (mean ± SEM, n = 4–5 each). Note that error bars are displayed, but often are hidden behind symbols.

(B) Giemsa-stained specimens of IgE-CAI skin lesions isolated 4 days postchallenge.

(C) The numbers of total cells and indicated cell types isolated from the ear skin on day 4 postchallenge are shown (mean ± SEM, n = 4–5 each). Data shown are representative of four independent experiments. *p < 0.05, **p < 0.01, ***p < 0.001.

was detected on CFSE-labeled cells infiltrating the skin lesions, regardless of the source of transferred cells (Figure 6C). On day 3 postchallenge, when the basophil infiltration reached a plateau (Figure 1C), a significant fraction of CFSE-labeled cells infiltrating the skin lesions expressed PD-L2 in mice that had received cells derived from wild-type but not *Il4ra*$^{-/-}$ mice (Figure 6C). Thus, monocytes recruited to the skin lesions acquired the PD-L2 expression in an IL-4 receptor (IL-4R)-dependent manner.

We then investigated whether basophils could contribute to this process. IgE-CAI was elicited in *Mcpt8*^{DTR} mice, and on day 2 postchallenge, CFSE-labeled CD115$^+$ bone marrow monocytes from wild-type mice were adoptively transferred to them, in conjunction with or without DT-mediated basophil ablation. The basophil ablation completely abolished the acquisition of PD-L2 expression by transferred monocytes infiltrating the skin lesions (Figure 6D). These results strongly suggested that blood-circulating monocytes acquire an M2-like phenotype after their recruitment to the IgE-CAI skin lesions, in response to basophil-derived IL-4.

Adoptive Transfer of Ly6C$^+$CCR2$^+$ Inflammatory Monocytes Dampens the Exacerbated IgE-CAI in *Ccr2*$^{-/-}$ Mice in an IL-4R-Dependent Manner

We next examined the functional consequence of the monocyte recruitment to the IgE-CAI skin lesions by means of adoptive transfer of wild-type monocytes to *Ccr2*$^{-/-}$ mice that display the exacerbated IgE-CAI. A single transfer of CD115$^+$ bone marrow monocytes at the time point of the antigen challenge, as shown in Figure 6A, showed no apparent impact on the ear swelling (data not show). We assumed that repeated transfer might be needed to reproduce the recruitment and accumulation of monocytes in the IgE-CAI skin lesions. Of note, four consecutive transfers of CD115$^+$ monocytes but not CD115$^-$ bone marrow cells dampened the exacerbated IgE-CAI in *Ccr2*$^{-/-}$ mice to the level observed in wild-type mice (Figure 7A), suggesting that CD115$^+$ bone marrow monocytes manifest an anti-inflammatory property after their recruitment to the skin lesion.

We then asked two questions. Are Ly6C$^+$Ly6G$^-$ inflammatory monocytes (rather than Ly6C$^-$ resident monocytes) that are recruited to and accumulate in the skin lesions indeed responsible for the negative regulation of IgE-CAI? Is the IL-4R-mediated acquisition of the M2-like phenotype by inflammatory monocytes associated with the regulation? To address these issues, Ly6C$^+$Ly6G$^-$ inflammatory monocytes were further purified from CD115$^+$ bone marrow cells, derived from either wild-type or *Il4ra*$^{-/-}$ mice, and directly transferred once into the ear dermis of *Ccr2*$^{-/-}$ mice where the antigens were administered (Figure 7B). The adoptive transfer of Ly6C$^+$Ly6G$^-$ inflammatory monocytes derived from wild-type but not *Il4ra*$^{-/-}$ mice dampened the exacerbated IgE-CAI. This strongly suggests that after the recruitment to the IgE-CAI skin lesions, CCR2$^+$Ly6C$^+$Ly6G$^-$ inflammatory monocytes acquired an M2-like phenotype through IL-4R and exerted an anti-inflammatory function to regulate the allergic inflammation.

DISCUSSION

Activated M2-type macrophages have been observed in a range of physiological and pathological processes, including Th2 cell-type immune responses (Kreider et al., 2007; Martinez et al., 2009; Murray and Wynn, 2011). However, the origin, differentiation pathway, and function of M2 macrophages have been ill defined, compared to those of M1 macrophages. In the present study, we have demonstrated a previously unappreciated cascade of monocyte-to-macrophage transition toward M2, being from proinflammatory to anti-inflammatory to dampen an allergic reaction. After recruitment to allergen-exposed skin, Ly6C$^+$CCR2$^+$ "inflammatory" monocytes acquired an M2-like phenotype and exerted an anti-inflammatory function in IgE-CAI, in response to IL-4 produced by antigen- and IgE-stimulated basophils. Accordingly, the failure in the recruitment

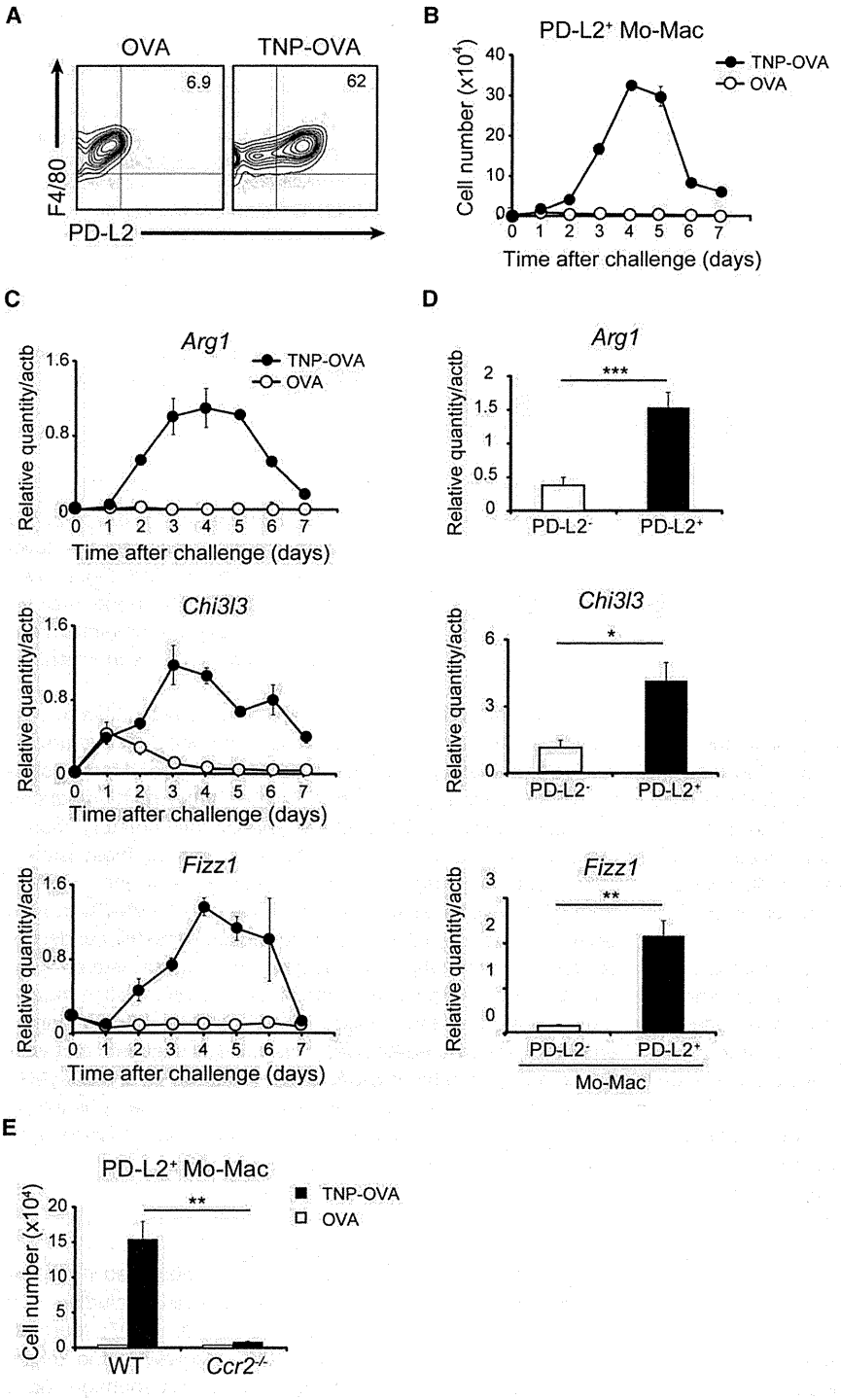

Figure 4. Monocytes-Macrophages Accumulating in the IgE-CAI Skin Lesions Display a Phenotype of M2-type Macrophages

(A–D) C57BL/6 mice were treated as in Figure 1 to induce IgE-CAI.

(A) The expression of PD-L2 on F4/80$^+$CD11b$^+$ SSC^{lo} monocytes-macrophages in the skin lesions of mice challenged with TNP-OVA or control OVA was examined on day 4 post-challenge.

(B and C) Time course of the PD-L2$^+$ monocytes-macrophage number (B, mean ± SEM, n = 3 each) and the expression of indicated mRNAs (C, mean ± SEM, n = 3 each) in the skin lesions of mice challenged with TNP-OVA (closed circles) or control OVA (open circles).

(D) The expression of indicated mRNAs in PD-L2$^-$ and PD-L2$^+$ monocytes-macrophages that were isolated on day 3 postchallenge from the ear skin of mice challenged with TNP-OVA (mean ± SEM, n = 6 each).

(E) Wild-type and *Ccr2*$^{-/-}$ BALB/c mice were treated as in Figure 3 to induce IgE-CAI. Data show the numbers of PD-L2$^+$ monocytes-macrophages that were isolated on day 4 postchallenge from the ear skin of mice challenged with TNP-OVA or control OVA (mean ± SEM, n = 4–5 each). Data shown are representative of at least three independent experiments. *p < 0.05, **p < 0.01, ***p < 0.001. See also Figures S1–S5.

of inflammatory monocytes in *Ccr2*$^{-/-}$ mice resulted in the exacerbation rather than alleviation of allergic inflammation, and adoptive transfer of CCR2$^+$ inflammatory monocytes normalized it. Thus, M2-like monocytes-macrophages derived from inflammatory monocytes appear to negatively regulate allergic inflammation in IgE-CAI.

Previous studies have shown two distinct modes of M2 generation. One is based on the observation during infection with *Listeria monocytogenes*. Ly6C$^{lo/-}$ resident monocytes recruited to the infection site turn on the expression of typical M2 marker genes, including *Arg1* and *Fizz1*, indicating their differentiation into M2 macrophages that probably contribute to tissue repair (Auffray et al., 2007). In contrast, Ly6C$^+$ inflammatory monocytes differentiate into dendritic cells that produce inflammatory mediators (Kurihara et al., 1997; Serbina et al., 2003). The other mode of M2 generation has been demonstrated in infection with helminth *Litomosoides sigmodontis*, in that M2 macrophages are generated through proliferation and alternative activation of tissue-resident macrophages rather than the recruitment of circulating monocytes (Jenkins et al., 2011). Our study on IgE-CAI has identified the third mode of M2 generation, in that Ly6C$^+$ inflammatory monocytes give rise to M2-type macrophages. The differentiation of inflammatory monocytes to M2 macrophages may not be restricted to allergic responses. A similar differentiation was suggested in experimental autoimmune encephalomyelitis, even though no direct evidence for this in vivo was provided (Denney et al., 2012).

The in vivo function of M2 macrophages has been less well characterized, compared to that of M1 macrophages, but has

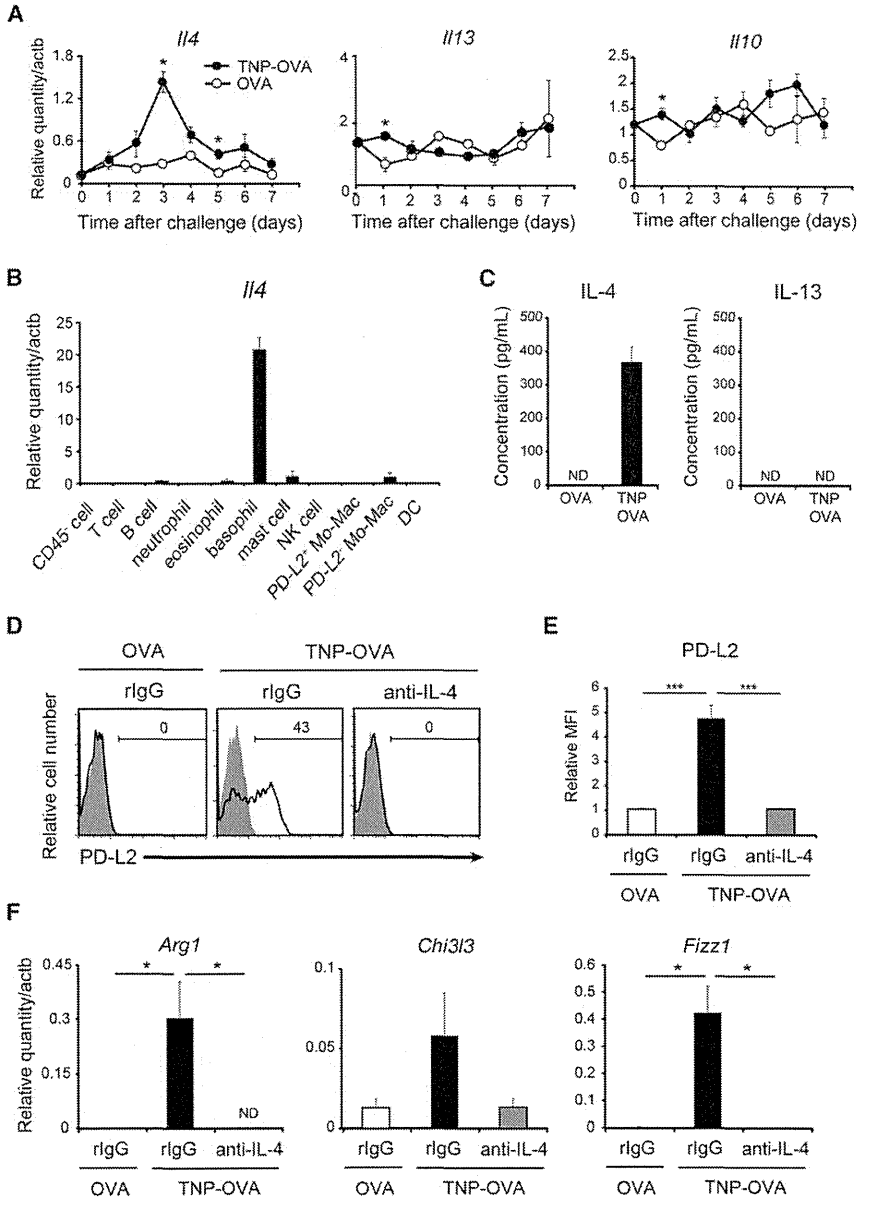

Figure 5. Basophil-Derived IL-4 Confers an M2-type Phenotype on Ly6C$^+$ Inflammatory Monocytes Ex Vivo

(A and B) C57BL/6 mice were treated as in Figure 1 to induce IgE-CAI. Time course of the expression of indicated mRNAs in the skin lesions of mice challenged with TNP-OVA (closed circles) or control OVA (open circles) is shown in (A) (mean ± SEM, n = 3 each). *p < 0.05. In (B), the indicated cell lineages were isolated on day 3 postchallenge from the skin lesions of mice challenged with TNP-OVA and subjected to quantitative RT-PCR for the analysis of *Il4* expression (mean ± SEM, n = 3 each).

(C) Basophils (2 × 10^5 cells/ml) enriched from bone marrow cells were sensitized ex vivo with anti-TNP IgE and then stimulated with TNP-OVA or control OVA at 37°C for 10 hr, and the concentration of IL-4 and IL-13 in their culture supernatants was determined by ELISA (mean ± SEM, n = 5 each). ND, not detectable.

(D–F) Ly6C$^+$ inflammatory monocytes were purified from C57BL/6 bone marrow cells and incubated at 37°C for 24 hr in the presence of anti-IL-4 or control rat IgG (rIgG), with the culture supernatants of basophils that had been stimulated as in (C).

(D and E) The cultured monocytes were subjected to flow cytometric analysis for PD-L2 expression. Representative staining profiles are shown in (D). Shaded histograms show control staining with isotype-matched antibody. All the data are summarized in (E) (mean ± SEM, n = 5–7 each), in that the relative mean fluorescence intensity (MFI) was calculated as MFI (PD-L2 staining)/MFI (control staining).

(F) The cultured monocytes were subjected to quantitative RT-PCR analysis for expression of indicated mRNAs (mean ± SEM, n = 5 each).

Data shown are representative of at least three independent experiments. *p < 0.05, ***p < 0.001.

been implicated in a variety of processes, including protection against parasitic infection, promoting Th2 cell-type immune responses, wound healing, tissue fibrosis, metabolic regulation, angiogenesis, and tumorigenesis (Kreider et al., 2007; Martinez et al., 2009; Murray and Wynn, 2011). The role of M2 macrophages in allergy and asthma has not been well understood, in contrast to the extensive study on its role in parasitic infections. Of note, in mice infected with helminth *Schistosoma mansoni*, M2 macrophages and their products have been shown to suppress rather than promote Th2 cell-type inflammation (Nair et al., 2009; Pesce et al., 2009). No such anti-inflammatory property of M2 macrophages was definitely demonstrated in allergic responses, as far as we aware. Instead, in mouse models of airway allergic inflammation, M2 macrophages reportedly contribute to the pathogenesis of disease, including promotion of inflammation (Ford et al., 2012; Kim et al., 2008; Kurowska-Stolarska et al., 2009; Melgert et al., 2010; Moreira et al., 2010; Nagarkar et al., 2010) and angiogenesis (Sun et al., 2008). Intriguingly, *Ccr2*$^{-/-}$ mice were reported to display enhanced airway allergic inflammation, but the underlying mechanism remains to be determined (Kim et al., 2001).

In the present study, we clearly demonstrated that M2-like monocytes-macrophages derived from inflammatory monocytes exert an anti-inflammatory function in IgE-CAI. Their absence or the failure in their conversion to M2 type resulted in the exacerbation of allergic inflammation. Thus, M2-like monocytes-macrophages appear to dampen excessive inflammation in IgE-CAI. It remains to be definitely demonstrated how they exert an anti-inflammatory function. Treatment of mice with an inhibitor of arginase-1 showed no apparent effect on IgE-CAI (data not show), although arginase-1 has been shown to suppress Th2 cell-type inflammation in helminth

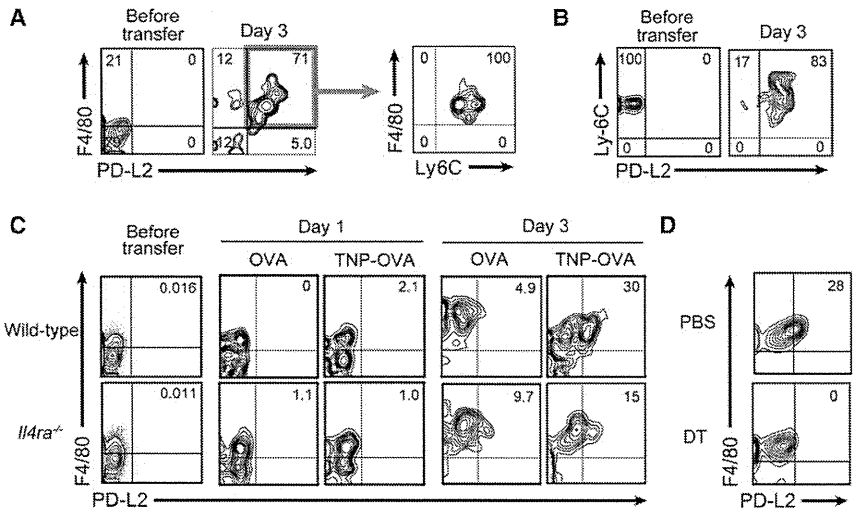

Figure 6. CD115$^+$ Monocytes Acquire PD-L2 Expression after Their Infiltration into the Skin Lesions, in a Manner Dependent on IL-4R and Basophils

(A and B) CD115$^+$ bone marrow cells isolated from BALB/c mice (A) or Ly6C$^+$Ly6G$^-$ inflammatory monocytes (purity > 99%) sorted from CD115$^+$ bone marrow cells (B) were labeled with CFSE and intravenously transferred (2 × 10^6 cells/mouse) into BALB/c mice that had been sensitized with anti-TNP IgE 1 day earlier. Recipient mice were challenged with intradermal administration of TNP-OVA immediately after the cell transfer. Flow cytometric analysis was performed for the surface expression of F4/80, PD-L2, and Ly6C in CFSE-labeled cells before the transfer and in those isolated from the TNP-OVA-injected skin on day 3 posttransfer.

(C) CD115$^+$ bone marrow cells were prepared from wild-type or *Il4ra*$^{-/-}$ mice, labeled with CFSE, and intravenously transferred (3 × 10^6 cells/mouse) into IgE-sensitized BALB/c mice, followed by the antigen challenge (TNP-OVA or control OVA) as in (A) and (B). Flow cytometric analysis was performed for the surface expression of F4/80 and PD-L2 in CFSE-labeled cells before the transfer (left) and in those isolated from the ear skin on day 1 and day 3 posttransfer (middle and right, respectively).

(D) *Mcpt8*^{DTR} C57BL/6 mice were sensitized with anti-TNP IgE and challenged with TNP-OVA as in Figure 1A to induce IgE-CAI. On day 2 postchallenge, the mice were treated with intravenous injection of CFSE-labeled CD115$^+$ bone marrow cells (1 × 10^7 cells/mouse) derived from wild-type mice, in conjunction with DT or control PBS. On day 4 postchallenge, the expression of F4/80 and PD-L2 on CFSE-labeled cells isolated from the ear skin was examined.

Data shown are representative of three independent experiments.

infection (Pesce et al., 2009). Notably, M2-like monocytes-macrophages infiltrating skin lesions of IgE-CAI express PD-L2, a ligand for the inhibitory receptor PD-1 (Loke and Allison, 2003). Blockade of PD-L2 with a specific antibody enhanced a Th2 cell-type response in helminth infection (Huber et al., 2010). However, our preliminary experiments with PD-L2 antibody suggested no apparent contribution of PD-L2 to the damping of allergic inflammation in IgE-CAI. In skeletal muscle injury, Ly6C$^+$ inflammatory monocytes are recruited and converted into "anti-inflammatory" macrophages that express IL-10 and transforming growth factor-β (TGF-β) (Arnold et al., 2007). In IgE-CAI, however, neither IL-10 nor TGF-β seems to be involved in damping inflammation in IgE-CAI (not all data shown). Of note, PD-L2$^+$ monocytes-macrophages accumulating in the IgE-CAI skin lesions expressed high amounts of a mannose receptor CD206 (Figure S6A), suggesting that they might have enhanced endocytic activity (Montaner et al., 1999). Indeed, PD-L2$^+$ monocytes-macrophages in the skin lesions showed a much higher extent of antigen uptake compared to PD-L2$^-$ monocytes-macrophages or other cell lineages including eosinophils and neutrophils (Figure S6B). This suggests that the failure in the generation of M2-like monocytes-macrophages may lead to the insufficient clearance of antigens in the skin lesions. Considering the fact that the extent and duration of the IgE-CAI reaction correlate well with the dose of antigens (Sato et al., 2003), the anti-inflammatory property of M2-like monocytes-macrophages could be attributed, at least in part, to their efficient uptake and clearance of antigens, making antigens unavailable for basophil activation.

Alternatively activated M2-type macrophages are typically generated by stimulation with the Th2 cell cytokines, IL-4 and IL-13, that can be produced by Th2 cells, natural killer T (NKT) cells, mast cells, eosinophils, basophils, and innate-type lymphoid cells (Paul and Zhu, 2010). Memory Th2 cells are the major source of Th2 cell cytokines for M2 generation in helminth infection (Anthony et al., 2006), whereas NKT cell-derived IL-4 is important for M2 generation in experimental autoimmune encephalomyelitis (Denney et al., 2012). In adipose tissues, eosinophil-derived IL-4 and IL-13 are crucial for M2 generation to maintain glucose homeostasis (Wu et al., 2011). In the present study, we demonstrated that basophil-derived IL-4 can act on inflammatory monocytes and convert them to anti-inflammatory M2-like monocytes-macrophages. Thus, basophils can contribute to the activation and differentiation of monocytes and macrophages, in addition to those of T and B cells as reported previously (Perrigoue et al., 2009; Sokol et al., 2008, 2009; Yoshimoto et al., 2009; Chen et al., 2009; Denzel et al., 2008). Of note, when stimulated ex vivo with IL-4, human CD14$^+$ monocytes display a phenotype characteristic for human M2-type macrophages, including upregulated expression of PD-L2 on their surface (Semnani et al., 2011). Given the fact that human basophils produce large quantities of Th2 cell cytokines as do murine basophils (Piccinni et al., 1991), it is plausible that basophils contribute to the generation of M2-type monocytes-macrophages in humans as observed in mice.

In conclusion, the present study demonstrated a previously unappreciated mode of monocyte-to-macrophage transition, that is, a conversion from inflammatory monocytes to anti-inflammatory M2-type monocytes-macrophages in an allergic response. In repeated infections with parasites, host animals often raise IgE against parasite antigens, and hence basophils can be stimulated with IgE plus antigens as seen in IgE-CAI (Karasuyama et al., 2011b; Voehringer, 2009). Moreover, basophils can be directly activated in an IgE-independent manner,

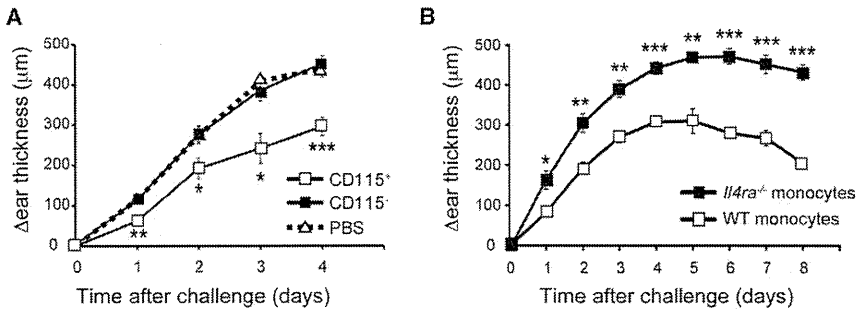

Figure 7. Adoptive Transfer of CCR2$^+$Ly6C$^+$ Inflammatory Monocytes from Wild-Type but Not *Il4ra*$^{-/-}$ Mice Normalizes the Exacerbated IgE-CAI in *Ccr2*$^{-/-}$ Mice

Ccr2$^{-/-}$ mice were treated as in Figure 3A to induce IgE-CAI.

(A) CD115$^+$ (open squares) or CD115$^-$ (closed squares) bone marrow cells from BALB/c mice or control PBS (open triangles) were intravenously administered to the mice four times (1 × 10^6 cells/injection/mouse), on days 0, 1, 2, and 3 post-challenge. Time course of ear swelling (Δear thickness) is shown (mean ± SEM, n = 3–5 each).

(B) Ly6C$^+$Ly6G$^-$ inflammatory monocytes (purity > 99%) sorted from bone marrow cells of wild-type (open squares) or *Il4ra*$^{-/-}$ (closed squares) mice were intradermally administered once (1 × 10^6 cells/site) in the ear of *Ccr2*$^{-/-}$ mice, in conjunction with administration of TNP-OVA or control OVA. Time course of ear swelling (Δear thickness) is shown (mean ± SEM, n = 4 each).

Data shown are representative of three independent experiments. *p < 0.05, **p < 0.01, ***p < 0.001. Note that error bars are displayed in all figures, but often are hidden behind symbols. See also Figures S6.

for example with certain proteases and pathogen products (Schroeder et al., 2001). Therefore, basophil-elicited M2 generation might be widely observed in various settings. Further studies will clarify their functional significance in each setting.

EXPERIMENTAL PROCEDURES

Mice

C57BL/6 and BALB/c mice were purchased from CLEA Japan. *Mcpt8*^{DTR} C57BL/6 (Wada et al., 2010), *Ccr2*$^{-/-}$ (Kuziel et al., 1997), and *Il4ra*$^{-/-}$ BALB/c (Noben-Trauth et al., 1997, 1999) mice were as described previously and maintained under specific-pathogen-free conditions in our animal facilities. All animal studies were approved by the Institutional Animal Care and Use Committee of Tokyo Medical and Dental University.

Induction of IgE-CAI

IgE-CAI was elicited as described previously (Mukai et al., 2005). In brief, mice were sensitized with intravenous injection of 300 μg of anti-TNP IgE, and on the following day challenged with an intradermal injection of 10 μg TNP_{12}-conjugated ovalbumin (OVA) and control OVA into the right and left ear, respectively. The value of Δear thickness, the differences in ear thickness (right − left) was calculated for the evaluation of inflammation.

Isolation of Bone Marrow Basophils and Monocytes

Basophils and monocytes were enriched from bone marrow cells via IMag system with biotinylated anti-CD49b and anti-CD115, respectively, followed by streptavidin-conjugated magnetic particles (BD PharMingen). Inflammatory monocytes were purified by sorting Ly6C^{hi}Siglec-F$^-$CD11c$^-$Ly6G$^-$ cells from the CD115$^+$ bone marrow cell population with FACSAria (BD Biosciences).

In Vitro Stimulation of Basophils and Monocytes

Basophils were stimulated for 10 hr with TNP_{12}-OVA or control OVA (300 ng/ml) after sensitization with TNP-specific IgE. The concentration of cytokines in culture supernatants was determined with Mouse IL-4 ELISA MAX Standard (Biolegend) for IL-4 and mouse Ready-Set-Go! ELISA kit (eBioscience) for IL-13. Monocytes were incubated for 24 hr with the culture supernatant of activated basophils in the presence or absence of anti-IL-4 or control rat IgG (20 μg/ml).

Ablation of Basophils

Mcpt8^{DTR} mice were treated once or twice with intravenous injection of diphtheria toxin (DT, Sigma-Aldrich, 500 ng/injection).

Statistical Analysis

Statistical analysis was performed with unpaired Student's t test. A p value <0.05 was considered statistically significant.

SUPPLEMENTAL INFORMATION

Supplemental Information includes Supplemental Experimental Procedures and six figures and can be found with this article online at http://dx.doi.org/10.1016/j.immuni.2012.11.014.

ACKNOWLEDGMENTS

We thank W.A. Kuziel (External Scientific Affairs, Daiichi Sankyo Group, Edison, NJ) for providing *Ccr2*$^{-/-}$ mice, D. Yamanaka and R. Matsunaga for technical support, and M. Miki for secretary assistance. This work was supported by a research grant from JST, CREST (to H.K.).

Received: August 4, 2012
Accepted: November 19, 2012
Published: February 21, 2013

REFERENCES

Anthony, R.M., Urban, J.F., Jr., Alem, F., Hamed, H.A., Rozo, C.T., Boucher, J.L., Van Rooijen, N., and Gause, W.C. (2006). Memory T(H)2 cells induce alternatively activated macrophages to mediate protection against nematode parasites. Nat. Med. *12*, 955–960.

Arnold, L., Henry, A., Poron, F., Baba-Amer, Y., van Rooijen, N., Plonquet, A., Gherardi, R.K., and Chazaud, B. (2007). Inflammatory monocytes recruited after skeletal muscle injury switch into antiinflammatory macrophages to support myogenesis. J. Exp. Med. *204*, 1057–1069.

Auffray, C., Fogg, D., Garfa, M., Elain, G., Join-Lambert, O., Kayal, S., Sarnacki, S., Cumano, A., Lauvau, G., and Geissmann, F. (2007). Monitoring of blood vessels and tissues by a population of monocytes with patrolling behavior. Science *317*, 666–670.

Auffray, C., Sieweke, M.H., and Geissmann, F. (2009). Blood monocytes: development, heterogeneity, and relationship with dendritic cells. Annu. Rev. Immunol. *27*, 669–692.

Biswas, S.K., and Mantovani, A. (2010). Macrophage plasticity and interaction with lymphocyte subsets: cancer as a paradigm. Nat. Immunol. *11*, 889–896.

Chen, K., Xu, W., Wilson, M., He, B., Miller, N.W., Bengtén, E., Edholm, E.S., Santini, P.A., Rath, P., Chiu, A., et al. (2009). Immunoglobulin D enhances immune surveillance by activating antimicrobial, proinflammatory and B cell-stimulating programs in basophils. Nat. Immunol. *10*, 889–898.

Denney, L., Kok, W.L., Cole, S.L., Sanderson, S., McMichael, A.J., and Ho, L.P. (2012). Activation of invariant NKT cells in early phase of experimental autoimmune encephalomyelitis results in differentiation of Ly6Chi inflammatory monocyte to M2 macrophages and improved outcome. J. Immunol. *189*, 551–557.

Denzel, A., Maus, U.A., Rodriguez Gomez, M., Moll, C., Niedermeier, M., Winter, C., Maus, R., Hollingshead, S., Briles, D.E., Kunz-Schughart, L.A.,

et al. (2008). Basophils enhance immunological memory responses. Nat. Immunol. *9*, 733–742.

Domínguez, P.M., and Ardavín, C. (2010). Differentiation and function of mouse monocyte-derived dendritic cells in steady state and inflammation. Immunol. Rev. *234*, 90–104.

Dunay, I.R., Damatta, R.A., Fux, B., Presti, R., Greco, S., Colonna, M., and Sibley, L.D. (2008). Gr1(+) inflammatory monocytes are required for mucosal resistance to the pathogen *Toxoplasma gondii*. Immunity *29*, 306–317.

Ford, A.Q., Dasgupta, P., Mikhailenko, I., Smith, E.M., Noben-Trauth, N., and Keegan, A.D. (2012). Adoptive transfer of IL-4Rα+ macrophages is sufficient to enhance eosinophilic inflammation in a mouse model of allergic lung inflammation. BMC Immunol. *13*, 6.

Galli, S.J. (2000). Mast cells and basophils. Curr. Opin. Hematol. *7*, 32–39.

Geissmann, F., Jung, S., and Littman, D.R. (2003). Blood monocytes consist of two principal subsets with distinct migratory properties. Immunity *19*, 71–82.

Geissmann, F., Manz, M.G., Jung, S., Sieweke, M.H., Merad, M., and Ley, K. (2010). Development of monocytes, macrophages, and dendritic cells. Science *327*, 656–661.

Gordon, S., and Taylor, P.R. (2005). Monocyte and macrophage heterogeneity. Nat. Rev. Immunol. *5*, 953–964.

Huber, S., Hoffmann, R., Muskens, F., and Voehringer, D. (2010). Alternatively activated macrophages inhibit T-cell proliferation by Stat6-dependent expression of PD-L2. Blood *116*, 3311–3320.

Ingersoll, M.A., Platt, A.M., Potteaux, S., and Randolph, G.J. (2011). Monocyte trafficking in acute and chronic inflammation. Trends Immunol. *32*, 470–477.

Jenkins, S.J., Ruckerl, D., Cook, P.C., Jones, L.H., Finkelman, F.D., van Rooijen, N., MacDonald, A.S., and Allen, J.E. (2011). Local macrophage proliferation, rather than recruitment from the blood, is a signature of TH2 inflammation. Science *332*, 1284–1288.

Karasuyama, H., Mukai, K., Obata, K., Tsujimura, Y., and Wada, T. (2011a). Nonredundant roles of basophils in immunity. Annu. Rev. Immunol. *29*, 45–69.

Karasuyama, H., Wada, T., Yoshikawa, S., and Obata, K. (2011b). Emerging roles of basophils in protective immunity against parasites. Trends Immunol. *32*, 125–130.

Kim, Y., Sung Ss, Kuziel, W.A., Feldman, S., Fu, S.M., and Rose, C.E., Jr. (2001). Enhanced airway Th2 response after allergen challenge in mice deficient in CC chemokine receptor-2 (CCR2). J. Immunol. *166*, 5183–5192.

Kim, E.Y., Battaile, J.T., Patel, A.C., You, Y., Agapov, E., Grayson, M.H., Benoit, L.A., Byers, D.E., Alevy, Y., Tucker, J., et al. (2008). Persistent activation of an innate immune response translates respiratory viral infection into chronic lung disease. Nat. Med. *14*, 633–640.

Kreider, T., Anthony, R.M., Urban, J.F., Jr., and Gause, W.C. (2007). Alternatively activated macrophages in helminth infections. Curr. Opin. Immunol. *19*, 448–453.

Kurihara, T., Warr, G., Loy, J., and Bravo, R. (1997). Defects in macrophage recruitment and host defense in mice lacking the CCR2 chemokine receptor. J. Exp. Med. *186*, 1757–1762.

Kurowska-Stolarska, M., Stolarski, B., Kewin, P., Murphy, G., Corrigan, C.J., Ying, S., Pitman, N., Mirchandani, A., Rana, B., van Rooijen, N., et al. (2009). IL-33 amplifies the polarization of alternatively activated macrophages that contribute to airway inflammation. J. Immunol. *183*, 6469–6477.

Kuziel, W.A., Morgan, S.J., Dawson, T.C., Griffin, S., Smithies, O., Ley, K., and Maeda, N. (1997). Severe reduction in leukocyte adhesion and monocyte extravasation in mice deficient in CC chemokine receptor 2. Proc. Natl. Acad. Sci. USA *94*, 12053–12058.

Loke, P., and Allison, J.P. (2003). PD-L1 and PD-L2 are differentially regulated by Th1 and Th2 cells. Proc. Natl. Acad. Sci. USA *100*, 5336–5341.

Martinez, F.O., Helming, L., and Gordon, S. (2009). Alternative activation of macrophages: an immunologic functional perspective. Annu. Rev. Immunol. *27*, 451–483.

Melgert, B.N., Oriss, T.B., Qi, Z., Dixon-McCarthy, B., Geerlings, M., Hylkema, M.N., and Ray, A. (2010). Macrophages: regulators of sex differences in asthma? Am. J. Respir. Cell Mol. Biol. *42*, 595–603.

Min, B., Brown, M.A., and Legros, G. (2012). Understanding the roles of basophils: breaking dawn. Immunology *135*, 192–197.

Montaner, L.J., da Silva, R.P., Sun, J., Sutterwala, S., Hollinshead, M., Vaux, D., and Gordon, S. (1999). Type 1 and type 2 cytokine regulation of macrophage endocytosis: differential activation by IL-4/IL-13 as opposed to IFN-gamma or IL-10. J. Immunol. *162*, 4606–4613.

Moreira, A.P., Cavassani, K.A., Hullinger, R., Rosada, R.S., Fong, D.J., Murray, L., Hesson, D.P., and Hogaboam, C.M. (2010). Serum amyloid P attenuates M2 macrophage activation and protects against fungal spore-induced allergic airway disease. J. Allergy Clin. Immunol. *126*, 712–721, e7.

Mosser, D.M., and Edwards, J.P. (2008). Exploring the full spectrum of macrophage activation. Nat. Rev. Immunol. *8*, 958–969.

Mukai, K., Matsuoka, K., Taya, C., Suzuki, H., Yokozeki, H., Nishioka, K., Hirokawa, K., Etori, M., Yamashita, M., Kubota, T., et al. (2005). Basophils play a critical role in the development of IgE-mediated chronic allergic inflammation independently of T cells and mast cells. Immunity *23*, 191–202.

Murray, P.J., and Wynn, T.A. (2011). Protective and pathogenic functions of macrophage subsets. Nat. Rev. Immunol. *11*, 723–737.

Nagarkar, D.R., Bowman, E.R., Schneider, D., Wang, Q., Shim, J., Zhao, Y., Linn, M.J., McHenry, C.L., Gosangi, B., Bentley, J.K., et al. (2010). Rhinovirus infection of allergen-sensitized and -challenged mice induces eotaxin release from functionally polarized macrophages. J. Immunol. *185*, 2525–2535.

Nair, M.G., Du, Y., Perrigoue, J.G., Zaph, C., Taylor, J.J., Goldschmidt, M., Swain, G.P., Yancopoulos, G.D., Valenzuela, D.M., Murphy, A., et al. (2009). Alternatively activated macrophage-derived RELM-alpha is a negative regulator of type 2 inflammation in the lung. J. Exp. Med. *206*, 937–952.

Noben-Trauth, N., Shultz, L.D., Brombacher, F., Urban, J.F., Jr., Gu, H., and Paul, W.E. (1997). An interleukin 4 (IL-4)-independent pathway for CD4+ T cell IL-4 production is revealed in IL-4 receptor-deficient mice. Proc. Natl. Acad. Sci. USA *94*, 10838–10843.

Noben-Trauth, N., Paul, W.E., and Sacks, D.L. (1999). IL-4- and IL-4 receptor-deficient BALB/c mice reveal differences in susceptibility to *Leishmania major* parasite substrains. J. Immunol. *162*, 6132–6140.

Obata, K., Mukai, K., Tsujimura, Y., Ishiwata, K., Kawano, Y., Minegishi, Y., Watanabe, N., and Karasuyama, H. (2007). Basophils are essential initiators of a novel type of chronic allergic inflammation. Blood *110*, 913–920.

Passlick, B., Flieger, D., and Ziegler-Heitbrock, H.W. (1989). Identification and characterization of a novel monocyte subpopulation in human peripheral blood. Blood *74*, 2527–2534.

Paul, W.E., and Zhu, J. (2010). How are T(H)2-type immune responses initiated and amplified? Nat. Rev. Immunol. *10*, 225–235.

Perrigoue, J.G., Saenz, S.A., Siracusa, M.C., Allenspach, E.J., Taylor, B.C., Giacomin, P.R., Nair, M.G., Du, Y., Zaph, C., van Rooijen, N., et al. (2009). MHC class II-dependent basophil-CD4+ T cell interactions promote T(H)2 cytokine-dependent immunity. Nat. Immunol. *10*, 697–705.

Pesce, J.T., Ramalingam, T.R., Mentink-Kane, M.M., Wilson, M.S., El Kasmi, K.C., Smith, A.M., Thompson, R.W., Cheever, A.W., Murray, P.J., and Wynn, T.A. (2009). Arginase-1-expressing macrophages suppress Th2 cytokine-driven inflammation and fibrosis. PLoS Pathog. *5*, e1000371.

Piccinni, M.P., Macchia, D., Parronchi, P., Giudizi, M.G., Bani, D., Alterini, R., Grossi, A., Ricci, M., Maggi, E., and Romagnani, S. (1991). Human bone marrow non-B, non-T cells produce interleukin 4 in response to cross-linkage of Fc epsilon and Fc gamma receptors. Proc. Natl. Acad. Sci. USA *88*, 8656–8660.

Sato, E., Hirahara, K., Wada, Y., Yoshitomi, T., Azuma, T., Matsuoka, K., Kubo, S., Taya, C., Yonekawa, H., Karasuyama, H., and Shiraishi, A. (2003). Chronic inflammation of the skin can be induced in IgE transgenic mice by means of a single challenge of multivalent antigen. J. Allergy Clin. Immunol. *111*, 143–148.

Schroeder, J.T., MacGlashan, D.W., Jr., and Lichtenstein, L.M. (2001). Human basophils: mediator release and cytokine production. Adv. Immunol. *77*, 93–122.

Seder, R.A., Paul, W.E., Dvorak, A.M., Sharkis, S.J., Kagey-Sobotka, A., Niv, Y., Finkelman, F.D., Barbieri, S.A., Galli, S.J., and Plaut, M. (1991). Mouse splenic and bone marrow cell populations that express high-affinity Fc epsilon receptors and produce interleukin 4 are highly enriched in basophils. Proc. Natl. Acad. Sci. USA *88*, 2835–2839.

Semnani, R.T., Mahapatra, L., Moore, V., Sanprasert, V., and Nutman, T.B. (2011). Functional and phenotypic characteristics of alternative activation induced in human monocytes by interleukin-4 or the parasitic nematode *Brugia malayi*. Infect. Immun. *79*, 3957–3965.

Serbina, N.V., and Pamer, E.G. (2006). Monocyte emigration from bone marrow during bacterial infection requires signals mediated by chemokine receptor CCR2. Nat. Immunol. *7*, 311–317.

Serbina, N.V., Salazar-Mather, T.P., Biron, C.A., Kuziel, W.A., and Pamer, E.G. (2003). TNF/iNOS-producing dendritic cells mediate innate immune defense against bacterial infection. Immunity *19*, 59–70.

Shi, C., and Pamer, E.G. (2011). Monocyte recruitment during infection and inflammation. Nat. Rev. Immunol. *11*, 762–774.

Siracusa, M.C., Comeau, M.R., and Artis, D. (2011). New insights into basophil biology: initiators, regulators, and effectors of type 2 inflammation. Ann. N Y Acad. Sci. *1217*, 166–177.

Sokol, C.L., Barton, G.M., Farr, A.G., and Medzhitov, R. (2008). A mechanism for the initiation of allergen-induced T helper type 2 responses. Nat. Immunol. *9*, 310–318.

Sokol, C.L., Chu, N.Q., Yu, S., Nish, S.A., Laufer, T.M., and Medzhitov, R. (2009). Basophils function as antigen-presenting cells for an allergen-induced T helper type 2 response. Nat. Immunol. *10*, 713–720.

Sun, Y., Wang, J., Li, H., and Han, X. (2008). Found in inflammatory zone 1 induces angiogenesis in murine models of asthma. Lung *186*, 375–380.

Tsou, C.L., Peters, W., Si, Y., Slaymaker, S., Aslanian, A.M., Weisberg, S.P., Mack, M., and Charo, I.F. (2007). Critical roles for CCR2 and MCP-3 in monocyte mobilization from bone marrow and recruitment to inflammatory sites. J. Clin. Invest. *117*, 902–909.

Voehringer, D. (2009). The role of basophils in helminth infection. Trends Parasitol. *25*, 551–556.

Voehringer, D. (2011). Basophils in allergic immune responses. Curr. Opin. Immunol. *23*, 789–793.

Wada, T., Ishiwata, K., Koseki, H., Ishikura, T., Ugajin, T., Ohnuma, N., Obata, K., Ishikawa, R., Yoshikawa, S., Mukai, K., et al. (2010). Selective ablation of basophils in mice reveals their nonredundant role in acquired immunity against ticks. J. Clin. Invest. *120*, 2867–2875.

Wu, D., Molofsky, A.B., Liang, H.E., Ricardo-Gonzalez, R.R., Jouihan, H.A., Bando, J.K., Chawla, A., and Locksley, R.M. (2011). Eosinophils sustain adipose alternatively activated macrophages associated with glucose homeostasis. Science *332*, 243–247.

Yoshimoto, T., Yasuda, K., Tanaka, H., Nakahira, M., Imai, Y., Fujimori, Y., and Nakanishi, K. (2009). Basophils contribute to T(H)2-IgE responses in vivo via IL-4 production and presentation of peptide-MHC class II complexes to CD4+ T cells. Nat. Immunol. *10*, 706–712.

nature medicine

ARTICLES

Thymic stromal lymphopoietin–elicited basophil responses promote eosinophilic esophagitis

Mario Noti[1,2,27], Elia D Tait Wojno[1,2,27], Brian S Kim[1–3], Mark C Siracusa[1,2], Paul R Giacomin[1,2,4], Meera G Nair[1,2,5], Alain J Benitez[6], Kathryn R Ruymann[7], Amanda B Muir[6], David A Hill[1,2,7], Kudakwashe R Chikwava[8], Amin E Moghaddam[9], Quentin J Sattentau[9], Aneesh Alex[10–12], Chao Zhou[10–12], Jennifer H Yearley[13], Paul Menard-Katcher[14], Masato Kubo[15,16], Kazushige Obata-Ninomiya[17,18], Hajime Karasuyama[17,18], Michael R Comeau[19], Terri Brown-Whitehorn[7], Rene de Waal Malefyt[20], Patrick M Sleiman[21–23], Hakon Hakonarson[21–23], Antonella Cianferoni[7], Gary W Falk[14,24,25], Mei-Lun Wang[6,24,25], Jonathan M Spergel[2,7,24,25] & David Artis[1,2,24–26]

Eosinophilic esophagitis (EoE) is a food allergy–associated inflammatory disease characterized by esophageal eosinophilia. Current management strategies for EoE are nonspecific, and thus there is a need to identify specific immunological pathways that could be targeted to treat this disease. EoE is associated with polymorphisms in the gene that encodes thymic stromal lymphopoietin (TSLP), a cytokine that promotes allergic inflammation, but how TSLP might contribute to EoE disease pathogenesis has been unclear. Here, we describe a new mouse model of EoE-like disease that developed independently of IgE, but was dependent on TSLP and basophils, as targeting TSLP or basophils during the sensitization phase limited disease. Notably, therapeutic TSLP neutralization or basophil depletion also ameliorated established EoE-like disease. In human subjects with EoE, we observed elevated *TSLP* expression and exaggerated basophil responses in esophageal biopsies, and a gain-of-function *TSLP* polymorphism was associated with increased basophil responses in patients with EoE. Together, these data suggest that the TSLP-basophil axis contributes to the pathogenesis of EoE and could be therapeutically targeted to treat this disease.

EoE is a food allergy–associated inflammatory disease that affects children and adults[1–3]. In industrialized countries, the incidence of EoE has increased dramatically in the past 30 years, resulting in a considerable public health and economic burden[2,4,5]. EoE is characterized by esophageal eosinophilia and inflammation and histological changes in the esophagus associated with stricture, dysphagia and food impaction[1–3]. Currently, treatment strategies for EoE are nonspecific and impose a burden on patients. Although swallowed topical steroids can be effective in limiting EoE-associated inflammation, there are concerns regarding the long-term use of steroids, particularly in children[2,6]. Adherence to an elemental diet that eliminates exposure to foods that trigger EoE results in resolution of symptoms in many patients; however, this approach requires disruptive changes in lifestyle and eating habits[2,6,7]. Thus, there is a need to identify new drug targets and more specific therapies[7]. The observations that immune suppression or removal of dietary trigger foods can ameliorate EoE symptoms indicate that EoE is a food antigen–driven

[1]Department of Microbiology, Perelman School of Medicine, University of Pennsylvania, Philadelphia, Pennsylvania, USA. [2]Institute for Immunology, Perelman School of Medicine, University of Pennsylvania, Philadelphia, Pennsylvania, USA. [3]Department of Dermatology, Perelman School of Medicine, University of Pennsylvania, Philadelphia, Pennsylvania, USA. [4]Centre for Biodiscovery and Molecular Development of Therapeutics, Queensland Tropical Health Alliance, James Cook University, Cairns, Queensland, Australia. [5]Division of Biomedical Sciences, School of Medicine, University of California-Riverside, Riverside, California, USA. [6]Division of Gastroenterology, Hepatology and Nutrition, Children's Hospital of Philadelphia, Philadelphia, Pennsylvania, USA. [7]Department of Pediatrics, Division of Allergy and Immunology, Children's Hospital of Philadelphia, Philadelphia, Pennsylvania, USA. [8]Department of Pathology and Laboratory Medicine, Children's Hospital of Philadelphia, Philadelphia, Pennsylvania, USA. [9]The Sir William Dunn School of Pathology, The University of Oxford, Oxford, UK. [10]Department of Electrical and Computer Engineering, Lehigh University, Bethlehem, Pennsylvania, USA. [11]Center for Photonics and Nanoelectronics, Lehigh University, Bethlehem, Pennsylvania, USA. [12]Bioengineering Program, Lehigh University, Bethlehem, Pennsylvania, USA. [13]Department of Pathology, Merck Research Laboratories, Palo Alto, California, USA. [14]Division of Gastroenterology, Perelman School of Medicine, University of Pennsylvania, Philadelphia, Pennsylvania, USA. [15]Laboratory for Cytokine Regulation, Research Center for Integrative Medical Science, RIKEN Yokohama Institute, Kanagawa, Japan. [16]Division of Molecular Pathology, Research Institute for Biomedical Science, Tokyo University of Science, Chiba, Japan. [17]Department of Immune Regulation, Tokyo Medical and Dental University Graduate School, Tokyo, Japan. [18]Japan Science and Technology Agency, Core Research for Evolutionary Science and Technology, Tokyo Medical and Dental University Graduate School, Tokyo, Japan. [19]Inflammation Research, Amgen, Seattle, Washington, USA. [20]Therapeutic Area Biology and Pharmacology, Merck Research Laboratories, Palo Alto, California, USA. [21]Center for Applied Genomics, Abramson Research Center, Children's Hospital of Philadelphia, Philadelphia, Pennsylvania, USA. [22]Division of Human Genetics, Abramson Research Center, Children's Hospital of Philadelphia, Philadelphia, Pennsylvania, USA. [23]Department of Pediatrics, Perelman School of Medicine, University of Pennsylvania, Philadelphia, Pennsylvania, USA. [24]Joint Penn-Children's Hospital of Philadelphia Center for Digestive, Liver and Pancreatic Medicine, Perelman School of Medicine, University of Pennsylvania and Children's Hospital of Philadelphia, Philadelphia, Pennsylvania, USA. [25]Center for Molecular Studies in Digestive and Liver Diseases, Department of Medicine, Division of Gastroenterology, Perelman School of Medicine, University of Pennsylvania, Philadelphia, Pennsylvania, USA. [26]Department of Pathobiology, School of Veterinary Medicine, University of Pennsylvania, Philadelphia, Pennsylvania, USA. [27]These authors contributed equally to this work. Correspondence should be addressed to D.A. (dartis@mail.med.upenn.edu).

Received 18 March; accepted 18 June; published online 21 July 2013; doi:10.1038/nm.3281

disease mediated by aberrant immune responses[1,2,8]. Therefore, targeting the dysregulated immunological pathways that underlie EoE could offer new treatment strategies for this disease.

Studies investigating the immunological mechanisms that mediate EoE have shown that various immune cell types, including eosinophils, mast cells, type 2 helper T (T_H2) cells that produce interleukin-4 (IL-4), IL-5, and IL-13, and IgE-producing B cells, may contribute to esophageal inflammation during EoE[1–3,9]. Further, recent work has shown that there is a strong association between a gain-of-function polymorphism in the gene that encodes the predominantly epithelial cell–derived cytokine TSLP and the development of EoE in children[10,11]. TSLP is associated with multiple allergic disorders[10–16] and is thought to promote allergic inflammation by activating dendritic cells, inducing T_H2 cell responses, supporting IgE production and eliciting the population expansion of phenotypically and functionally distinct basophils[12,17–21]. However, whether TSLP directly promotes inflammatory responses associated with EoE and the mechanisms by which polymorphisms in *TSLP* and increased TSLP expression may contribute to the pathogenesis of EoE in patients has been unknown.

RESULTS

A new mouse model of experimental EoE-like disease

To investigate whether TSLP directly promotes EoE disease pathogenesis, we developed a new mouse model of EoE-like disease that is associated with exaggerated TSLP production. Multiple studies in mouse models and humans suggest that sensitization to food allergens may occur at sites where the skin barrier is disrupted, such as atopic dermatitis lesions[22–24]. Thus, we employed a model in which mice were epicutaneously sensitized to a food antigen, ovalbumin (OVA), on a developing atopic dermatitis–like skin lesion induced by topical treatment with the vitamin D analog MC903 (**Fig. 1a**). Consistent with previous reports[17,25–27], wild-type (WT) BALB/c mice treated epicutaneously with the vitamin D analog MC903 showed increased TSLP expression in the skin compared to ethanol vehicle–treated control mice (**Fig. 1b**). Epicutaneous sensitization to and subsequent oral challenge with OVA resulted in the development of experimental EoE-like disease that was characterized by inflammation, edema and eosinophilia in the esophagus, as measured histologically and quantified by enumeration of eosinophils per high-power field (HPF) (**Fig. 1c,d**). Flow cytometric analysis (**Fig. 1e,f**) and immunofluorescence staining (**Fig. 1g**) also demonstrated that there was an accumulation of eosinophils in esophageal tissues of mice with EoE-like disease, and electron microscopic (EM) analysis revealed the presence of degranulated eosinophils in these tissues (**Fig. 1h**). We also observed significantly higher expression of genes that encode T_H2 cytokines and the basophil-specific protease *Mcpt8* and a trend toward increased *Tslp* expression in esophageal tissues of mice with EoE-like disease compared to control mice (**Fig. 1i**). Further, we observed a similar

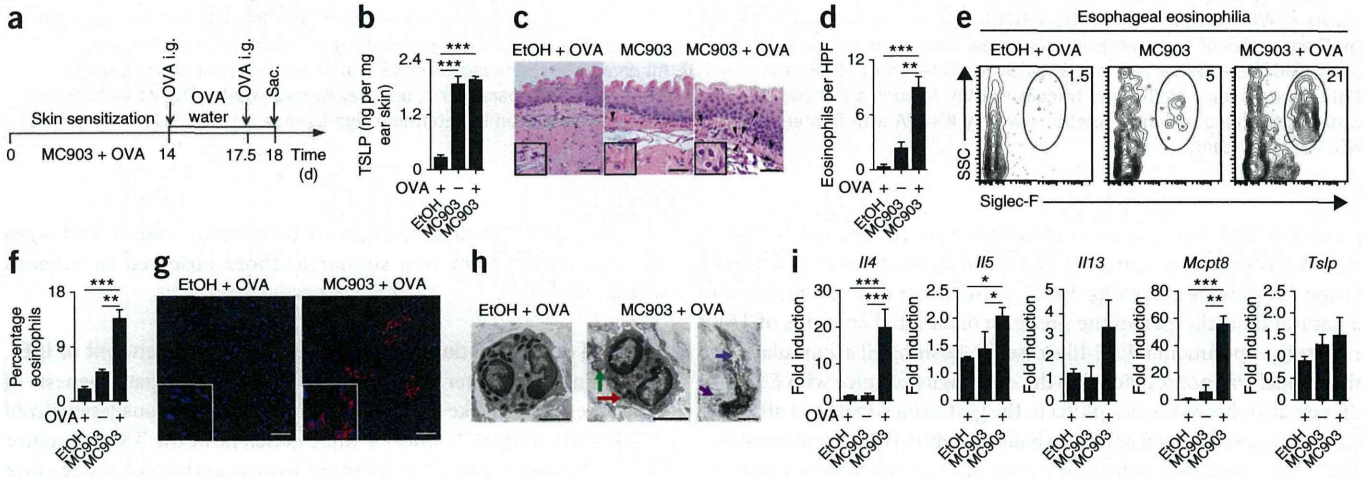

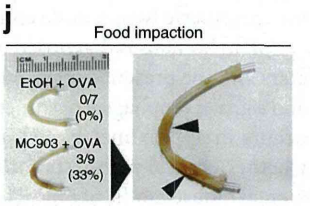

Figure 1 Experimental mouse model of EoE-like disease. (**a**) Schematic of EoE-like disease mouse model in which WT BALB/c mice are epicutaneously sensitized for 14 d with OVA on a developing atopic dermatitis–like skin lesion, challenged intragastrically (i.g.) with OVA on days 14 and 17.5 and sacrificed (sac.) at day 18. (**b**) TSLP (ng per mg of ear skin) expression in supernatants of overnight-cultured skin (ears) measured by ELISA. Data are from one experiment (EtOH + OVA, $n = 3$; MC903, $n = 3$; MC903 + OVA, $n = 4$) and are representative of three independent replicates. EtOH, ethanol. (**c**) Histological sections (H&E staining) from the esophagus. Arrowheads identify tissue-infiltrating eosinophils. Scale bar, 25 μm. Insets: ×4 magnification of whole image focusing on eosinophils. (**d**) Number of eosinophils per HPF in the esophagus. (**e**) Representative flow cytometry plots showing frequencies of eosinophils in esophageal tissues. Data in **c**–**e** are from one experiment (EtOH + OVA, $n = 3$; MC903, $n = 3$; MC903 + OVA, $n = 4$) and are representative of three or more independent replicates. (**f**) Frequencies of eosinophils in esophageal tissues, as measured by flow cytometry. Data are from three pooled experiments (EtOH + OVA, $n = 7$; MC903, $n = 8$; MC903 + OVA, $n = 11$). (**g**) Immunofluorescence staining for eosinophils (Siglec-F–specific mAb, red) in esophageal tissues. Counterstaining with DAPI (blue). Scale bar, 25 μm. Images are representative of two controls and three EoE-like disease samples. Insets: ×4 magnification of whole image focusing on eosinophils. (**h**) Representative EM image of an eosinophil in the esophagus of control mice with intact granules with electron dense cores (left) or degranulating eosinophils in MC903 + OVA–treated mice (right), showing loss of electron density in granule cores (red arrow), granule extrusion channels (blue arrow) and complete loss of granule contents (green arrow) into the extracellular matrix (purple arrow). Scale bar, 2 μm. (**i**) mRNA expression of T_H2 cytokines (*Il4*, *Il5*, *Il13*), the basophil-specific protease *Mcpt8* and *Tslp* in the esophagus. Data depicted are from one experiment (EtOH + OVA, $n = 3$; MC903, $n = 3$; MC903 + OVA, $n = 4$) and are representative of three independent replicates. *y* axis shows fold induction compared to controls (see Online Methods). (**j**) Representative images of esophagi, with incidence of impaction. Arrowheads identify impacted food. Data depicted are from two pooled experiments (EtOH + OVA, $n = 7$, MC903 + OVA, $n = 9$). All parameters were assessed 12 h post-final oral antigen challenge. Data in **a**–**i** are from mice challenged twice with OVA, and data in **j** are from mice challenged six times with OVA. Results are shown as mean ± s.e.m., and a nonparametric, one-way Kruskal-Wallis analysis of variance (ANOVA) with Dunn's *post hoc* testing was used to determine significance. $^*P \le 0.05$; $^{**}P \le 0.01$; $^{***}P \le 0.001$.

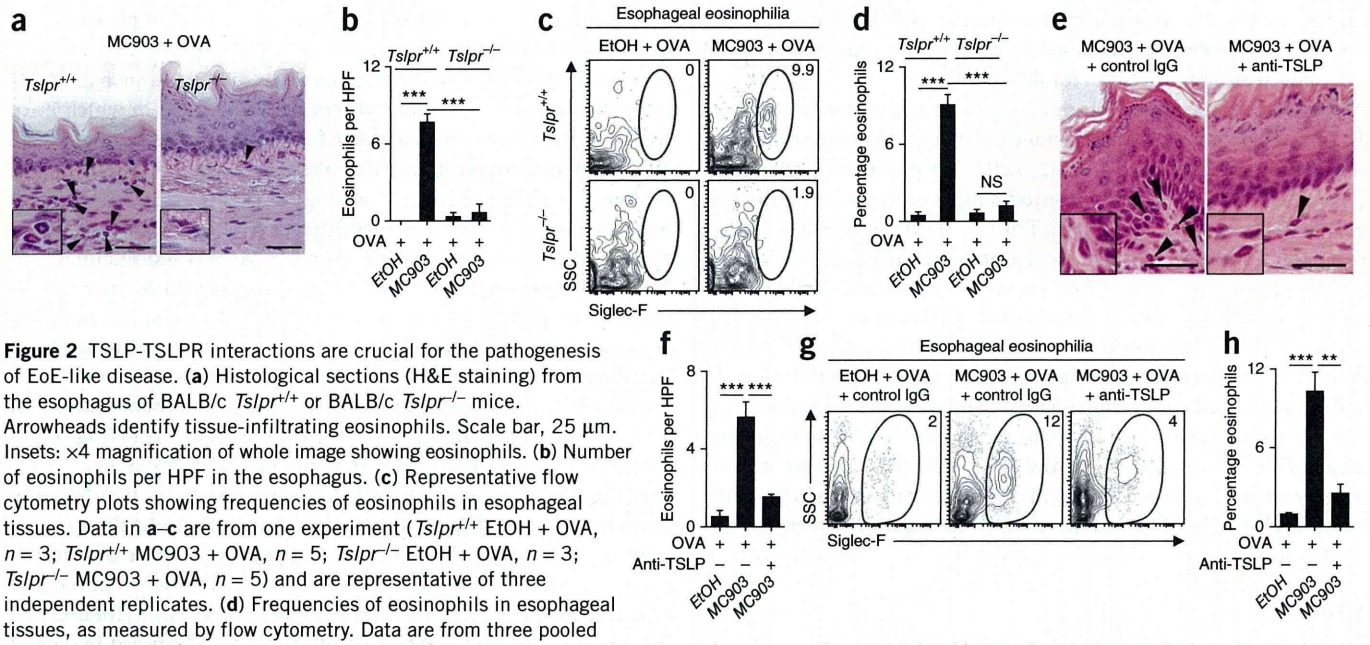

Figure 2 TSLP-TSLPR interactions are crucial for the pathogenesis of EoE-like disease. (**a**) Histological sections (H&E staining) from the esophagus of BALB/c *Tslpr*$^{+/+}$ or BALB/c *Tslpr*$^{-/-}$ mice. Arrowheads identify tissue-infiltrating eosinophils. Scale bar, 25 μm. Insets: ×4 magnification of whole image showing eosinophils. (**b**) Number of eosinophils per HPF in the esophagus. (**c**) Representative flow cytometry plots showing frequencies of eosinophils in esophageal tissues. Data in **a**–**c** are from one experiment (*Tslpr*$^{+/+}$ EtOH + OVA, $n = 3$; *Tslpr*$^{+/+}$ MC903 + OVA, $n = 5$; *Tslpr*$^{-/-}$ EtOH + OVA, $n = 3$; *Tslpr*$^{-/-}$ MC903 + OVA, $n = 5$) and are representative of three independent replicates. (**d**) Frequencies of eosinophils in esophageal tissues, as measured by flow cytometry. Data are from three pooled experiments (*Tslpr*$^{+/+}$ EtOH + OVA, $n = 5$; *Tslpr*$^{+/+}$ MC903 + OVA, $n = 11$; *Tslpr*$^{-/-}$ EtOH + OVA, $n = 5$; *Tslpr*$^{-/-}$ MC903 + OVA, $n = 12$). (**e**) Histological sections (H&E staining) from the esophagus of WT BALB/c mice treated with an isotype control or TSLP-specific mAb (anti-TSLP). Arrowheads identify tissue-infiltrating eosinophils. Scale bar, 50 μm. Insets: ×4 magnification of whole image showing eosinophils. (**f**) Number of eosinophils per HPF in the esophagus. (**g**) Representative flow cytometry plots showing frequencies of eosinophils in esophageal tissues. Data in **e**–**g** are from one experiment (EtOH + OVA + IgG, $n = 3$; MC903 + OVA + IgG, $n = 3$; MC903 + OVA + anti-TSLP mAb, $n = 3$) and are representative of three independent replicates. (**h**) Frequencies of eosinophils in esophageal tissues, as measured by flow cytometry. Data are from three pooled experiments (EtOH + OVA +IgG, $n = 5$; MC903 + OVA + IgG, $n = 9$; MC903 + OVA + anti-TSLP mAb, $n = 10$). All parameters were assessed 12 h after final oral antigen challenge. Data are from mice challenged twice with OVA. Results are shown as mean ± s.e.m., and a nonparametric, one-way Kruskal-Wallis ANOVA with Dunn's *post hoc* testing or a nonparametric, two-way ANOVA with Bonferroni's *post hoc* testing were used to determine significance. $^{**}P \leq 0.01$; $^{***}P \leq 0.001$. NS, not significant.

pattern of EoE-like disease in mice that were epicutaneously sensitized to crude peanut extract (CPE) on an atopic dermatitis–like skin lesion (**Supplementary Fig. 1a–c**), confirming that sensitization to a natural food allergen in the presence of elevated amounts of TSLP results in experimental EoE-like disease. Eosinophil accumulation in this model was not restricted to the esophagus, as mice with EoE-like disease also showed eosinophilia in the gastrointestinal tract after epicutaneous sensitization and oral challenge with OVA (**Supplementary Fig. 1d,e**) associated with antigen-specific T_H2 cytokine responses in the mesenteric lymph node and spleen (**Supplementary Fig. 1f,g**).

EoE in humans is diagnosed on the basis of immunological parameters and the presence of physiological changes in esophageal tissue and signs of esophageal dysfunction, including food impaction, which occurs in approximately 40% of patients with EoE[1–3,28]. To assess whether clinical manifestations of EoE were present in the experimental mouse model of EoE-like disease, we challenged mice that had existing EoE-like disease repeatedly with OVA to induce prolonged esophageal inflammation. Although analysis using optical coherence tomography (OCT), which allows for high-resolution imaging of live biological tissues based on optical scattering[29,30], revealed that EoE-like disease was characterized by minimal changes in the thickness of the esophageal epithelium, (**Supplementary Fig. 2a,b**), prolonged esophageal inflammation was associated with food impaction in the esophagus. Approximately 30% of fasted mice with EoE-like disease exhibited food impaction at the time of killing, but we never observed food impaction in the esophagus of control (ethanol)-treated mice (**Fig. 1j**). Collectively, these data indicate that this new model of EoE-like disease is characterized by a number of immunological and pathophysiological changes in esophageal tissues and signs of esophageal dysfunction similar to those observed in humans with EoE[1–3,31–34].

EoE-like disease is dependent on TSLP but independent of IgE

To determine whether TSLP directly promotes the pathogenesis of experimental EoE-like disease in mice, we epicutaneously sensitized WT BALB/c (*Tslpr*$^{+/+}$) mice or mice deficient in the TSLP receptor (TSLPR) (*Tslpr*$^{-/-}$) to OVA followed by oral antigen challenge (see **Fig. 1a**). Whereas sensitized and challenged *Tslpr*$^{+/+}$ mice showed esophageal eosinophilia and associated inflammation, *Tslpr*$^{-/-}$ mice did not develop esophageal eosinophilia (**Fig. 2a–d**). Using an alternative approach to abrogate TSLP signaling, we found that multiple systemic treatments with a monoclonal antibody (mAb) that neutralizes TSLP during epicutaneous sensitization with OVA in WT BALB/c mice also limited eosinophil infiltration in the esophagus after oral challenge (**Fig. 2e–h**).

To test whether TSLP was sufficient for the development of EoE-like disease during epicutaneous sensitization, we intradermally injected mice with exogenous recombinant TSLP (rTSLP) in the presence or absence of OVA and challenged them orally (**Supplementary Fig. 3a**). Mice sensitized to OVA in the presence of rTSLP also showed esophageal eosinophilia after oral challenge compared to mice treated with OVA alone or rTSLP alone (**Supplementary Fig. 3b**). In a complementary approach, *Tslpr*$^{+/+}$ mice were treated with control antibody or a TSLP-specific mAb, and *Tslpr*$^{-/-}$ mice were sensitized with OVA on tape-stripped skin (**Supplementary Fig. 3c**). Tape-stripping was associated with elevated local TSLP production following physical

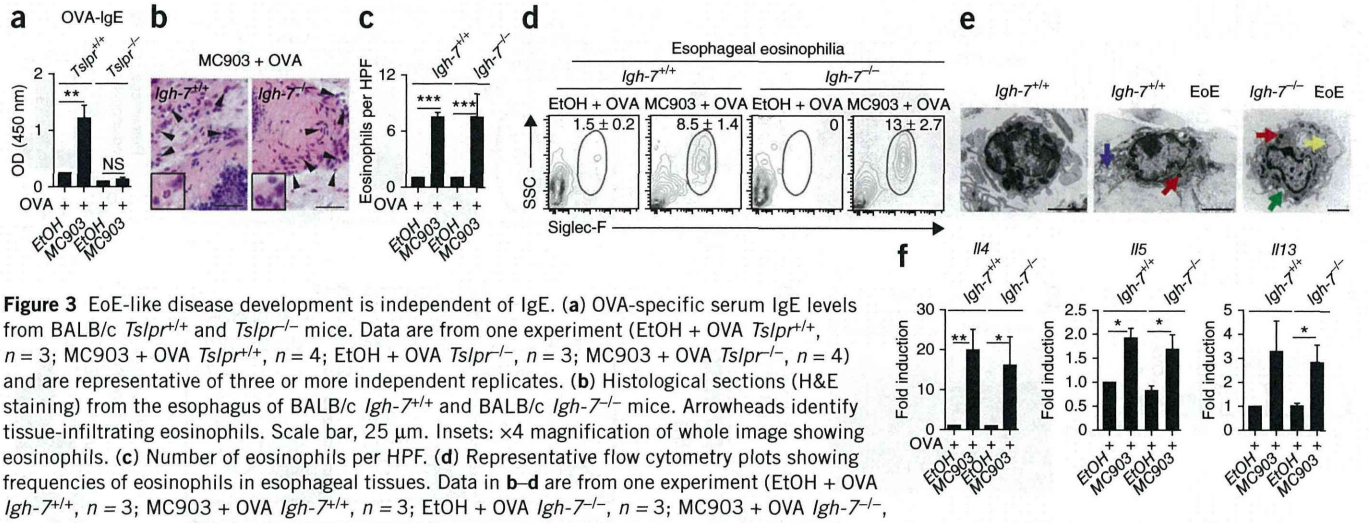

Figure 3 EoE-like disease development is independent of IgE. (**a**) OVA-specific serum IgE levels from BALB/c *Tslpr*$^{+/+}$ and *Tslpr*$^{-/-}$ mice. Data are from one experiment (EtOH + OVA *Tslpr*$^{+/+}$, $n = 3$; MC903 + OVA *Tslpr*$^{+/+}$, $n = 4$; EtOH + OVA *Tslpr*$^{-/-}$, $n = 3$; MC903 + OVA *Tslpr*$^{-/-}$, $n = 4$) and are representative of three or more independent replicates. (**b**) Histological sections (H&E staining) from the esophagus of BALB/c *Igh-7*$^{+/+}$ and BALB/c *Igh-7*$^{-/-}$ mice. Arrowheads identify tissue-infiltrating eosinophils. Scale bar, 25 μm. Insets: ×4 magnification of whole image showing eosinophils. (**c**) Number of eosinophils per HPF. (**d**) Representative flow cytometry plots showing frequencies of eosinophils in esophageal tissues. Data in **b**–**d** are from one experiment (EtOH + OVA *Igh-7*$^{+/+}$, $n = 3$; MC903 + OVA *Igh-7*$^{+/+}$, $n = 3$; EtOH + OVA *Igh-7*$^{-/-}$, $n = 3$; MC903 + OVA *Igh-7*$^{-/-}$, $n = 4$) and are representative of three or more independent replicates. (**e**) Representative EM image of an eosinophil in the esophagus of control *Igh-7*$^{+/+}$ mice with intact granules with electron-dense cores (left) or degranulating eosinophils in MC903 + OVA treated *Igh-7*$^{+/+}$ (middle) or *Igh-7*$^{-/-}$ (right) mice in various stages of degranulation, with loss of electron density in granule cores (red arrows), formation of granule extrusion channels (blue arrow), complete loss of granule contents (green arrow) and formation of lipid vesicles (yellow arrow). Scale bar, 2 μm. (**f**) mRNA expression of T_H2 cytokines in the esophagus. Data are from one experiment (EtOH + OVA *Igh-7*$^{+/+}$, $n = 3$; MC903 + OVA *Igh-7*$^{+/+}$, $n = 3$; EtOH + OVA *Igh-7*$^{-/-}$, $n = 3$; MC903 + OVA *Igh-7*$^{-/-}$, $n = 3$) and are representative of two independent replicates. *y* axis shows fold induction compared to controls (see Online Methods). All parameters were assessed 12 h after final oral antigen challenge. Data are from mice challenged twice with OVA. Results are shown as mean ± s.e.m., and a nonparametric, two-way ANOVA with Bonferroni's *post hoc* testing was used to determine significance. $^*P \leq 0.05$, $^{**}P \leq 0.01$; $^{***}P \leq 0.001$. NS, not significant.

perturbation of the skin barrier (**Supplementary Fig. 3d** and ref. 35). Whereas *Tslpr*$^{+/+}$ mice treated with control antibody that were sensitized to OVA on tape-stripped skin showed esophageal eosinophilia after oral antigen challenge, *Tslpr*$^{+/+}$ mice treated with a TSLP-specific mAb and *Tslpr*$^{-/-}$ mice did not develop esophageal eosinophilia (**Supplementary Fig. 3e,f**). Finally, we assessed the contribution of TSLP to the development of clinical signs of EoE-like disease. Repeated challenge with OVA following sensitization in the presence of MC903 was not associated with changes in the thickness of the esophageal epithelium. However, prolonged esophageal inflammation was associated with an increased incidence of food impaction in the esophagus in *Tslpr*$^{+/+}$ but not *Tslpr*$^{-/-}$ mice (**Supplementary Fig. 4a,b**). Collectively, these data indicate that TSLP-TSLPR interactions are necessary and sufficient for the development of experimental EoE-like disease in mice.

TSLP-TSLPR interactions are known to promote the production of IgE[36,37], a key mediator of allergic inflammation[38], and class-switched B cells have been observed in the esophagus of patients with EoE[9,39,40]. In addition, MC903-induced TSLP expression was associated with high amounts of systemic OVA-specific IgE (**Fig. 3a**), suggesting that TSLP-dependent EoE-like disease in mice might be IgE dependent. To directly test this, we epicutaneously sensitized IgE-sufficient WT BALB/c (*Igh-7*$^{+/+}$) mice and IgE-deficient (*Igh-7*$^{-/-}$) mice to OVA in the presence of MC903. Following oral challenge with antigen, both *Igh-7*$^{+/+}$ and *Igh-7*$^{-/-}$ mice showed equivalent EoE-like disease, characterized by esophageal inflammation, elevated tissue eosinophilia (**Fig. 3b–d**), the presence of degranulated eosinophils in the esophagus (**Fig. 3e**) and significant increases in gene expression of T_H2 cytokines in esophageal tissues (**Fig. 3f**). These data demonstrate that EoE-like disease can occur in an IgE-independent manner and are consistent with recent findings from clinical studies suggesting that treatment with an IgE-specific mAb does not ameliorate EoE in most patients[41–44]. Together, these data indicate that manipulation of the IgE pathway may not be an effective therapeutic approach for the treatment of EoE.

EoE-like disease depends on basophils

In addition to its role in promoting B cell and IgE responses, TSLP expression is associated with the selective expansion of a distinct population of basophils[17,18]. These data suggest that basophils may contribute to TSLP-dependent, IgE-independent EoE-like disease in mice. Consistent with this hypothesis, MC903-induced expression of TSLP in the skin was associated with TSLP-dependent, IgE-independent systemic basophil responses (**Supplementary Fig. 5a,b**). To assess whether basophils contribute to the development of experimental EoE-like disease, we employed an established genetic approach to deplete basophils *in vivo*. C57BL/6 mice in which the diphtheria toxin receptor (DTR) is exclusively expressed by basophils (Baso-DTR$^+$ mice)[17,19,45] and DTR-negative littermate controls (Baso-DTR$^-$ mice) were epicutaneously sensitized and orally challenged with OVA while being treated with diphtheria toxin (**Fig. 4a**). Consistent with results observed in BALB/c mice (**Fig. 1b**), we observed increased local and systemic TSLP production in C57BL/6 Baso-DTR$^-$ and Baso-DTR$^+$ mice sensitized to OVA in the context of MC903 treatment (data not shown). Notably, whereas Baso-DTR$^-$ mice that were epicutaneously sensitized and orally challenged with OVA showed high frequencies of eosinophils in the esophagus, depletion of basophils in Baso-DTR$^+$ mice (**Supplementary Fig. 5c**) led to a reduction in esophageal eosinophilia (**Fig. 4b–e**) and a reduction in expression of genes related to T_H2 cytokine responses (**Supplementary Fig. 6a–c**).

Using an alternative approach, we treated epicutaneously sensitized and orally challenged WT BALB/c mice with a mAb specific for CD200R3 (Ba103) to deplete basophils[46] (**Fig. 4f**). Mice in which basophils were depleted during sensitization (**Supplementary Fig. 5d**) showed a reduced accumulation of eosinophils in the esophagus compared to control mAb–treated mice after oral challenge with OVA (**Fig. 4g–j**). Collectively, these

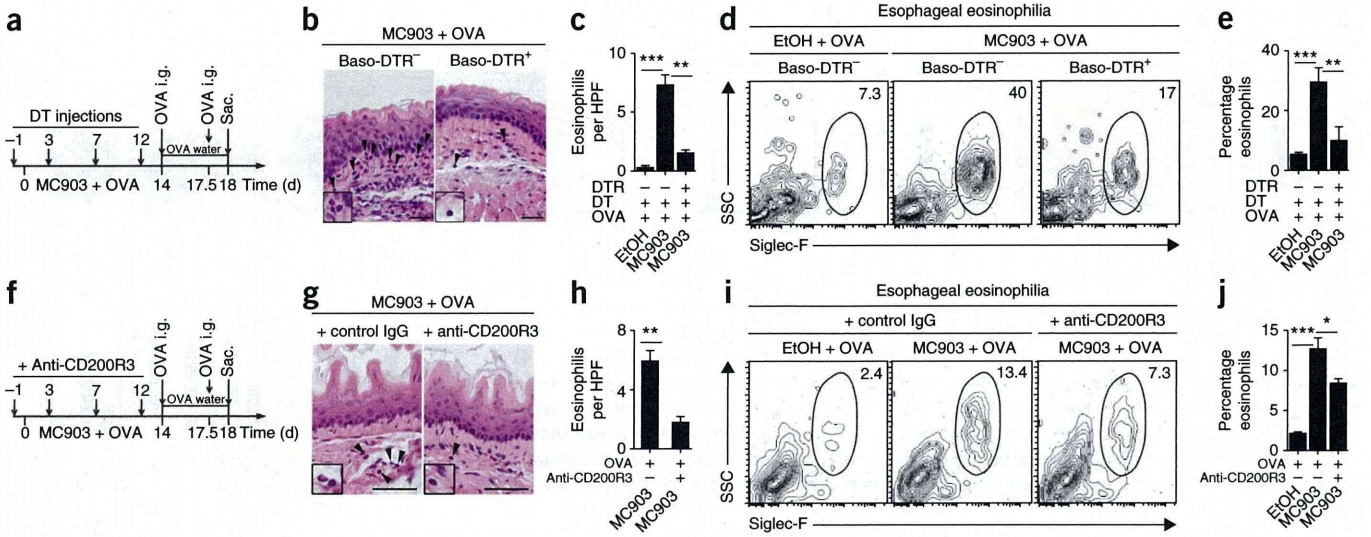

Figure 4 Basophils promote EoE-like disease. (**a**) Schematic of *in vivo* basophil depletion strategy. C57BL/6 (Baso-DTR$^-$) or Baso-DTR$^+$ mice were treated with diphtheria toxin (DT) during the course of epicutaneous sensitization. (**b**) Histological sections (H&E staining) from the esophagus. Arrowheads identify tissue-infiltrating eosinophils. Scale bar, 25 μm. Insets: ×4 magnification of whole image showing eosinophils. (**c**) Number of eosinophils per HPF in the esophagus. (**d**) Representative flow cytometry plots showing frequencies of eosinophils in esophageal tissues. Data in **b**–**d** are from one experiment (Baso-DTR$^-$ EtOH + OVA, $n = 3$; Baso-DTR$^-$ MC903 + OVA, $n = 3$; Baso-DTR$^+$ MC903 + OVA, $n = 4$) and are representative of three independent replicates. (**e**) Frequencies of eosinophils in esophageal tissues, as measured by flow cytometry. Data depicted are from three pooled experiments (Baso-DTR$^-$ EtOH + OVA, $n = 7$; Baso-DTR$^-$ MC903 + OVA, $n = 10$; Baso-DTR$^+$ MC903 + OVA, $n = 11$). (**f**) Schematic of *in vivo* basophil depletion strategy using CD200R3-specific mAb (anti-CD200R3) in WT BALB/c mice. (**g**) Histological sections (H&E staining) from the esophagus. Arrowheads identify tissue-infiltrating eosinophils. Scale bar, 50 μm. Insets: ×4 magnification of whole image showing eosinophils. (**h**) Number of eosinophils per HPF in the esophagus. (**i**) Representative flow cytometry plots showing frequencies of eosinophils in esophageal tissues. Data in **g**–**i** are from one experiment (EtOH + OVA + IgG, $n = 3$; MC903 + OVA + IgG, $n = 3$; MC903 + OVA + anti-CD200R3 mAb, $n = 4$) and are representative of three independent replicates. (**j**) Frequencies of eosinophils in esophageal tissues, as measured by flow cytometry. Data are from three pooled experiments (EtOH + OVA + IgG, $n = 8$; MC903 + OVA + IgG, $n = 9$; MC903 + OVA + anti-CD200R3 mAb, $n = 10$). All parameters were assessed 12 h after final oral antigen challenge. Data are from mice challenged twice with OVA. Results are shown as mean ± s.e.m., and a nonparametric, two-tailed Mann-Whitney *t*-test or a nonparametric, one-way Kruskal-Wallis ANOVA with Dunn's *post hoc* testing were used to determine significance. $^*P \le 0.05$; $^{**}P \le 0.01$; $^{***}P \le 0.001$.

results indicate that basophils are major contributors to the pathogenesis of experimental EoE-like disease in mice and may represent a new therapeutic target to treat this disease in patients.

TSLP or basophils can be targeted to treat EoE-like disease

As TSLP and basophils were required during sensitization for the development of EoE-like disease in mice, we next tested whether the TSLP-basophil pathway could be therapeutically targeted to treat established EoE-like disease. First, we sensitized and challenged mice with OVA to establish EoE-like disease and then treated them systemically with either an isotype control or a neutralizing TSLP-specific mAb during repeated antigen challenge (**Fig. 5a**). Whereas mice with established EoE-like disease treated with a control antibody showed esophageal eosinophilia, mice that were treated with a TSLP-specific mAb had decreased esophageal eosinophilia, as measured histologically (**Fig. 5b**). Flow cytometric analysis also revealed that the total immune cell infiltrate and esophageal eosinophilia were significantly reduced in mice treated with a TSLP-specific mAb compared to mice treated with a control mAb (**Fig. 5c,d**).

To test whether basophils contributed to the maintenance of EoE-like disease, we treated mice with established EoE-like disease with an isotype control or basophil-depleting CD200R3-specific mAb during repeated OVA challenge (**Fig. 5e**). Similar to the results observed after neutralization of TSLP, specific depletion of basophils resulted in decreased esophageal eosinophilia, as measured histologically (**Fig. 5f**), and flow cytometric analysis showed a reduction in total immune cell infiltrate and eosinophil numbers in the esophagus (**Fig. 5g,h**). To test whether neutralization of TSLP or depletion of basophils was also associated with a resolution of signs of esophageal dysfunction, we treated mice with established EoE-like disease with a control antibody, TSLP-specific mAb, or CD200R3-specific mAb and assessed them for the incidence of food impaction. Whereas we observed food impaction in about 30% of mice treated with a control antibody, we did not observe food impaction in mice in which TSLP or basophil responses were blocked (**Fig. 5i**). Taken together, these data demonstrate that TSLP neutralization or basophil depletion can be used to ameliorate inflammation and clinical symptoms of established experimental EoE-like disease in mice.

The TSLP-basophil axis is associated with EoE in humans

The roles of TSLP and basophils in experimental EoE-like disease in mice (**Figs. 2** and **4**) and the established association between a gain-of-function polymorphism in *TSLP* and EoE in human pediatric subjects[10,11] prompted us to hypothesize that the TSLP-basophil pathway may contribute to the pathogenesis of EoE in humans. To assess whether the TSLP-basophil axis is active in human subjects with EoE, we examined TSLP expression and basophil responses in esophageal biopsies from a cohort of pediatric subjects. We stratified this patient population on the basis of the number of eosinophils counted in histologic sections from esophageal biopsies into the following groups: (i) control subjects without EoE, (ii) subjects with active EoE (≥15 eosinophils per HPF) and (iii) subjects with inactive EoE (<15 eosinophils per HPF and a prior clinical history of active EoE) (**Fig. 6a**). In agreement with previous studies[10,11],

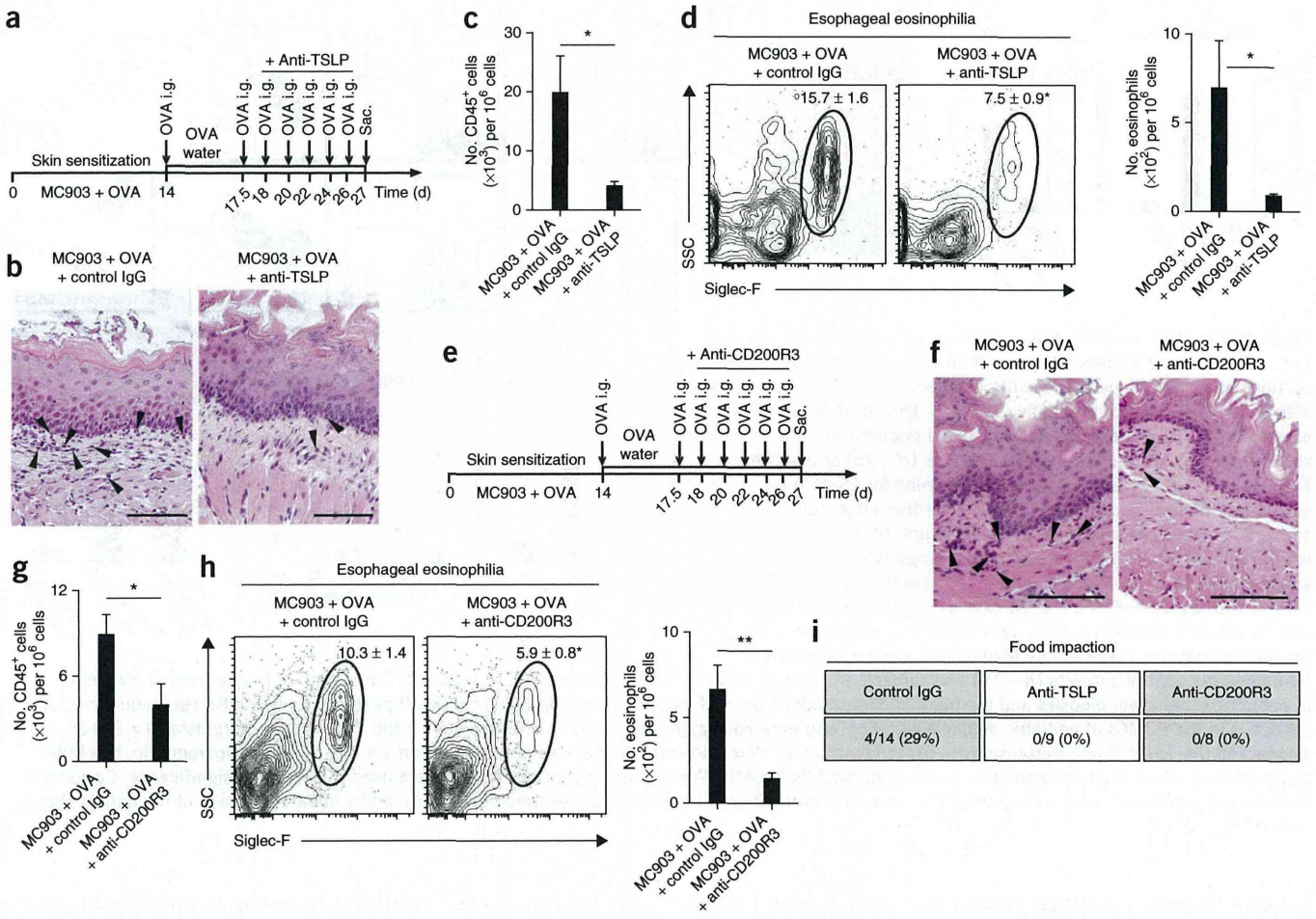

Figure 5 Neutralization of TSLP or depletion of basophils ameliorates established EoE-like disease. (**a**) Schematic of treatment with TSLP-specific mAb in WT BALB/c mice with established EoE-like disease. (**b**) Histological sections (H&E staining) from the esophagus. Arrowheads identify tissue-infiltrating eosinophils. Scale bar, 50 μm. (**c**) Frequencies of CD45$^+$ cells in esophageal tissues, as measured by flow cytometry. (**d**) Representative flow cytometry plots showing frequencies and total numbers of eosinophils in esophageal tissues. Data in **b**–**d** are from one experiment (MC903 + OVA + IgG, $n = 5$; MC903 + OVA + anti-TSLP mAb, $n = 5$) and are representative of three independent replicates. (**e**) Schematic of CD200R3-specific mAb basophil-depletion strategy in WT BALB/c mice in established EoE-like disease. (**f**) Histological sections (H&E staining) from the esophagus. Arrowheads identify tissue-infiltrating eosinophils. Scale bar, 50 μm. (**g**) Frequencies of CD45$^+$ cells in esophageal tissues, as measured by flow cytometry. (**h**) Representative flow cytometry plots showing frequencies and total numbers of eosinophils in esophageal tissues. Data in **f**–**h** are from one experiment (MC903 + OVA + IgG, $n = 4$; MC903 + OVA + anti-CD200R3 mAb, $n = 5$) and are representative of three independent replicates. (**i**) Quantified incidence of food impaction. All parameters were assessed 12 h after final oral antigen challenge. Data are from mice challenged repeatedly with OVA. Results are shown as mean ± s.e.m., and a nonparametric, two-tailed Mann-Whitney *t*-test was used to determine significance. $^*P \leq 0.05$; $^{**}P \leq 0.01$.

TSLP expression in esophageal biopsies was higher in subjects with active EoE compared to control subjects or subjects with inactive EoE (**Fig. 6b**). Immunohistochemical staining revealed that stratified squamous epithelial cells showed positive staining for TSLP in esophageal biopsies from subjects with active EoE (**Fig. 6c**). We then used flow cytometric analysis to identify and quantify the inflammatory cell infiltrate in biopsies. Notably, we observed higher frequencies of cells with a phenotype consistent with that of basophils (lin$^-$CD49b$^+$FcεRI$^+$c-kit$^-$2D7$^+$) in esophageal biopsies from subjects with active EoE compared to those from control subjects or subjects with inactive EoE (**Fig. 6d,e**). Further, the frequency of basophils positively correlated (Spearman $r = 0.6638$) with the number of eosinophils counted per HPF in histological sections of esophageal biopsies (**Fig. 6f**). Additionally, we were able to stratify a cohort of adult subjects on the basis of the number of eosinophils counted in histologic sections (**Supplementary Fig. 7a**). Consistent with results observed in pediatric subjects (**Fig. 6d–f**), adult subjects with active EoE had a higher (although not statistically significant) frequency of basophils in the esophageal biopsy, as measured using flow cytometry, that positively correlated (Spearman $r = 0.5282$) with the number of eosinophils counted per HPF in histological sections (**Supplementary Fig. 7b,c**). Collectively, these data indicate for the first time, to our knowledge, that the TSLP-basophil axis is associated with active EoE in pediatric and adult subjects.

These findings, coupled with the association between the development of EoE and a previously identified gain-of-function polymorphism in *TSLP* associated with *TSLP* overexpression (*TSLP*^{risk})[10], suggested that there may be an association between the *TSLP*^{risk} polymorphism and enhanced basophil responses in human subjects with EoE. To directly test this, we assessed a separate cohort of pediatric subjects with active or inactive EoE genotyped for the presence of the *TSLP*^{risk} polymorphism for basophil frequencies among peripheral blood mononuclear cells (PBMCs). Subjects who were homozygous or heterozygous for the *TSLP*^{risk} polymorphism had significantly higher

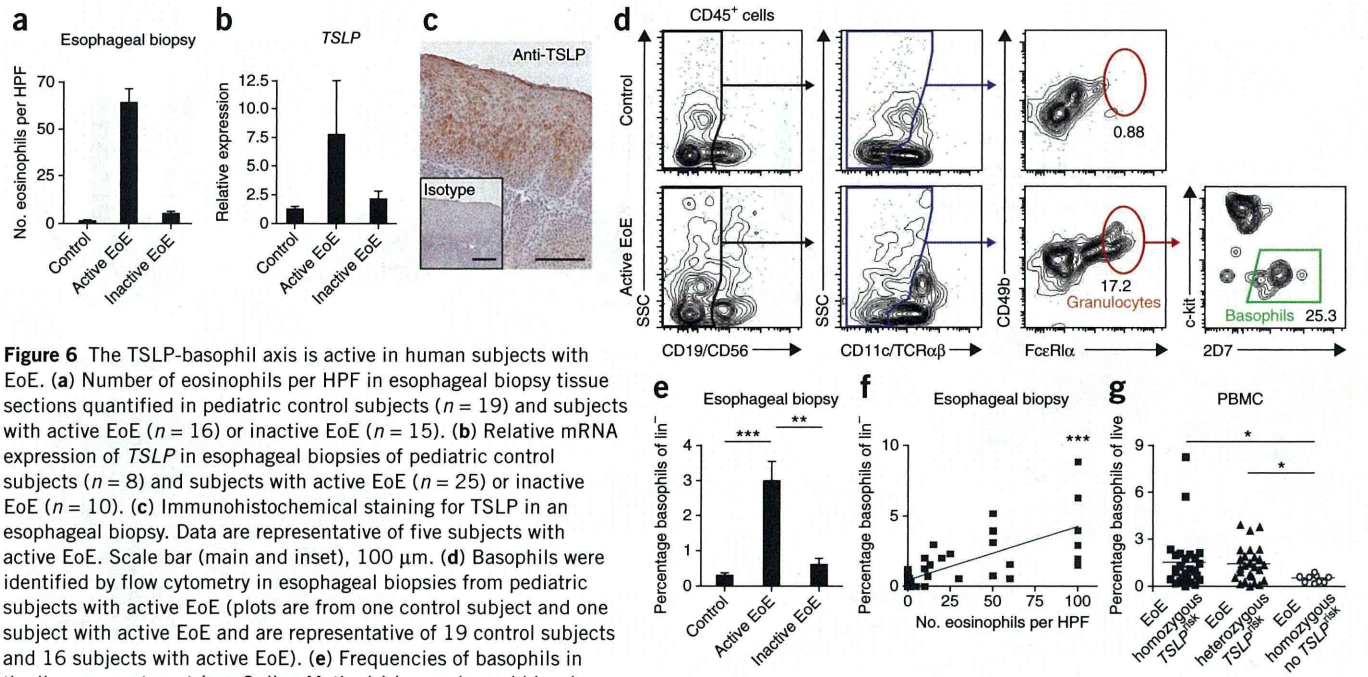

Figure 6 The TSLP-basophil axis is active in human subjects with EoE. (**a**) Number of eosinophils per HPF in esophageal biopsy tissue sections quantified in pediatric control subjects ($n = 19$) and subjects with active EoE ($n = 16$) or inactive EoE ($n = 15$). (**b**) Relative mRNA expression of *TSLP* in esophageal biopsies of pediatric control subjects ($n = 8$) and subjects with active EoE ($n = 25$) or inactive EoE ($n = 10$). (**c**) Immunohistochemical staining for TSLP in an esophageal biopsy. Data are representative of five subjects with active EoE. Scale bar (main and inset), 100 μm. (**d**) Basophils were identified by flow cytometry in esophageal biopsies from pediatric subjects with active EoE (plots are from one control subject and one subject with active EoE and are representative of 19 control subjects and 16 subjects with active EoE). (**e**) Frequencies of basophils in the lin$^-$ compartment (see Online Methods) in esophageal biopsies from pediatric control subjects ($n = 19$) and subjects with active EoE ($n = 16$) or inactive EoE ($n = 15$). (**f**) Correlation of frequencies of basophils in pediatric esophageal biopsies and the number of eosinophils per HPF observed histologically ($n = 50$) (Spearman $r = 0.6638$). (**g**) Frequencies of basophils in the PBMCs of pediatric subjects with EoE who were homozygous ($n = 26$) or heterozygous for the *TSLP*^{risk} polymorphism ($n = 26$) or who lacked the *TSLP*^{risk} polymorphism ($n = 9$), as identified by flow cytometry. All data are shown as mean ± s.e.m., and a nonparametric, two-tailed Mann-Whitney *t*-test or a nonparametric, one-way Kruskal-Wallis ANOVA with Dunn's *post hoc* testing were used to determine significance. Correlation analysis was performed using a nonparametric Spearman correlation (sensitivity analyses were performed), and a linear regression of the data is shown. $^*P \le 0.05$; $^{**}P \le 0.01$; $^{***}P \le 0.001$.

basophil frequencies in their PBMCs than subjects with EoE who did not carry the *TSLP*^{risk} polymorphism (**Fig. 6g**), which suggests a genetic link between a gain-of-function *TSLP* polymorphism, increased peripheral basophil responses and EoE. As with most human inflammatory diseases such as asthma, inflammatory bowel disease and multiple sclerosis[47–50], the development of EoE probably involves a complex interplay of genetic and environmental factors. However, these data suggest a model in which patients that carry the *TSLP*^{risk} polymorphism have a predisposition toward *TSLP* overexpression and associated peripheral basophilia that may increase the likelihood of developing EoE after encounter with trigger antigens (**Supplementary Fig. 8**).

DISCUSSION

Here we describe a new mouse model in which epicutaneous sensitization to a model food antigen followed by oral antigen challenge results in EoE-like disease. We demonstrate that TSLP and basophils, but not IgE, are required for the development of experimental EoE-like disease in mice and that antibody-mediated neutralization of TSLP or depletion of basophils is effective in preventing the development of experimental EoE-like disease. Targeting TSLP or basophils was also effective in treating established EoE-like disease in mice. In addition, we identify for the first time the presence of enhanced basophil responses in the esophageal biopsy tissue of human subjects with EoE and a genetic link between a gain-of-function polymorphism in *TSLP* and increased peripheral basophil responses.

Although all experimental model systems have limitations and do not recapitulate the diversity of symptoms reported in humans, the model of EoE-like disease we report here is associated with several characteristics of EoE in humans, including esophageal eosinophilia and associated esophageal dysfunction. In addition, this model is also characterized by gastrointestinal eosinophilia and systemic T_H2 cytokine responses. EoE in humans is defined as a disease associated with eosinophilia in the esophagus. However, patients with EoE often suffer from coexisting allergic disorders such as atopic dermatitis, allergic rhinitis, asthma or intestinal food allergy[2,7,51]. These observations suggest that a subset of individuals with EoE with coexisting allergic diseases may present with manifestations of allergic disease at tissue sites outside of the esophagus[52]. Thus, the mouse model of EoE-like disease we describe may recapitulate a pan-allergic disease state present in some humans who have EoE and suffer from additional allergic diseases. Although EoE-like disease in this model develops independently of IgE and is dependent on TSLP and basophils, further studies will be required to investigate whether the gastrointestinal eosinophilia in this model is dependent on IgE or TSLP-elicited basophils.

Previous studies in mouse models and humans have identified various immunological factors that are associated with EoE[1–3,31–34,53–58]. However, recent clinical trials that have targeted some of these factors, including IgE and IL-5, have failed to ameliorate symptoms of disease[2,41,42,44,59,60], suggesting that these factors may not be essential for the pathogenesis of EoE. The demonstration that EoE-like disease in mice can develop independently of IgE but is dependent on TSLP and basophils may explain why previous clinical trials employing other candidate biologic therapies have not been successful. The identification of a role for TSLP and basophils in experimental EoE-like disease in mice, coupled with the association between TSLP and basophil responses and EoE in humans, indicate